ISTANBUL TECHNICAL UNIVERSITY ★ GRADUATE SCHOOL

DEVELOPMENT OF A GAS SENSING NANOFIBROUS MEMBRANE FOR ASTHMA DETECTION

M.Sc. THESIS

Ari HAKGÖR

Department of Textile Engineering

Innovative Technical Textiles Programme

JANUARY 2024

ISTANBUL TECHNICAL UNIVERSITY ★ GRADUATE SCHOOL

DEVELOPMENT OF A GAS SENSING NANOFIBROUS MEMBRANE FOR ASTHMA DETECTION

M.Sc. THESIS

Ari HAKGÖR
(503201820)

Department of Textile Engineering

Innovative Technical Textiles Programme

Thesis Advisor: Prof. Dr. Selin Hanife ERYÜRÜK

JANUARY 2024

İSTANBUL TEKNİK ÜNİVERSİTESİ ★ LİSANSÜSTÜ EĞİTİM ENSTİTÜSÜ

ASTIM HASTALIĞININ TAYİNİ İÇİN GAZ ALGILAYICI NANOLİFLİ MEMBRAN GELİŞTİRİLMESİ

YÜKSEK LİSANS TEZİ

Ari HAKGÖR
(503201820)

Tekstil Mühendisliği Anabilim Dalı

Yenilikçi Teknik Tekstiller Programı

Tez Danışmanı: Prof. Dr. Selin Hanife ERYÜRÜK

OCAK 2024

Ari HAKGÖR, a M.Sc. student of ITU Graduate School student ID 503201820, successfully defended the thesis entitled “DEVELOPMENT OF A GAS SENSING NANOFIBROUS MEMBRANE FOR ASTHMA DETECTION”, which he prepared after fulfilling the requirements specified in the associated legislations, before the jury whose signatures are below.

Thesis Advisor :	Prof. Dr. Selin Hanife ERYÜRÜK İstanbul Technical University	……..
Jury Members :	Prof. Dr. Hale KARAKAŞ İstanbul Technical University	……..
	Doç. Dr. Nuray KIZILDAĞ Gebze Technical University	……..

Date of Submission : 15 December 2023
Date of Defense : 9 January 2024

FOREWORD

This thesis would not have been written without the help of several individuals who extended their valuable assistance and guidance to whom I am greatly indebted.

First and foremost, I offer my utmost gratitude to my advisor Professor Selin Hanife ERYÜRÜK and responsible professors during my Erasmus+ mobility period in JUNIA HEI (École des hautes études d'ingénieur), Assoc. Prof. Elham MOHSENZADEH and Assoc. Prof. Hayriye GIDIK VANDERBERCK, for their supervision, valuable advice and guidance throughout my graduate studies; without their constant support, kindness and patience this study would not have been completed.

I gratefully acknowledge thesis jury members Professor Hale KARAKAŞ and Associate Prof. Nuray KIZILDAĞ for their invaluable comments and helpful suggestions; they provided crucial contributions to this thesis.

I am grateful to Professor Gülay ÖZCAN with whom I had the privilege of working on a project together. Her guidance and shared experiences have been invaluable.

Many thanks go in particular to İTÜ Erasmus Office and JUNIA HEI International Relations Office for their sincere and unending support during my Erasmus+ mobility.

I would also like to thank my dear friends Ayşenur, Kâmil, Işıl, Ayşe Zeyneb, Göknil, Halenur and Dr. Pelin ALTAY for their sincere support throughout my experimental work.

Last but not least, I would like to thank everybody who one way or another contributed to the successful realization of this thesis.

December 2023

Ari HAKGÖR
(Chemist)

TABLE OF CONTENTS

Page

ACRONYMS/ABBREVIATION

CO	**:** Carbon monoxide
CO_2	**:** Carbon dioxide
H_2	**:** Hydrogen gas
H_2O	**:** Water
H_2S	**:** Hydrogen sulfide
O_2	**:** Oxygen gas
O_3	**:** Ozone
NaCl	**:** Sodium chloride
Na_2CO_3	**:** Sodium carbonate
NO	**:** Nitric oxide
NO_2	**:** Nitrogen dioxide
N_2O	**:** Nitrous oxide (dinitrogen oxide)
N_2O_3	**:** Dinitrogen trioxide
NO_x	**:** Nitrogen oxides
TiO_2	**:** Titanium dioxide
SnO_2	**:** Tin dioxide
WO_3	**:** Tungsten trioxide
$ZnCl_2$	**:** Zinc chloride
$ZnCO_3$	**:** Zinc carbonate
$Zn(NO_3)_2$	**:** Zinc nitrate
$ZnSO_4$	**:** Zinc sulphate
ZnO	**:** Zinc oxide
$Zn(OH)_2$	**:** Zinc hydroxide
$Zn(CH_3COO)_2$ or $Zn(OAc)_2$	**:** Zinc acetate
$Zn(OAc)_2 \cdot 2H_2O$	**:** Zinc acetate dihydrate
$[Zn(OH)_4]^{2-}$	**:** Tetrahydroxozincate ion
pH	**:** Potential (or power) of hydrogen
PVA	**:** Polyvinyl alcohol
SEM	**:** Scanning electron microscope
TGA	**:** Thermogravimetric analysis

SYMBOLS

ppt	**:** Parts per trillion
ppm	**:** Parts per million
ppb	**:** Parts per billion
w/v	**:** Weight per volume
M_w	**:** Molecular weight
cm	**:** Centimeter(s)
mm	**:** Millimeter(s)
µm	**:** Micometer(s)
nm	**:** Nanometer(s)
g	**:** gram(s)
$\dot{\gamma}$	**:** Shear rate
Q	**:** Flow rate
r	**:** Radius of the needle
V	**:** Volt
kV	**:** Kilovolt
s	**:** Second(s)
h	**:** Hour(s)
mL/min	**:** Millimeter per minute
uL/min	**:** Microliter per minute
s^{-1}	**:** Reciprocal second
rpm	**:** Revolutions per minute
mN/m	**:** Millinewton/meter
Pa.s	**:** Pascal-second
°C	**:** Degree Celsius
°C/min	**:** Degree Celsius per minute
µS/cm	**:** MicroSiemens/cm
S (solubility)	**:** Mol of substance per kg of water

LIST OF TABLES

Page

LIST OF FIGURES

Page

DEVELOPMENT OF A GAS SENSING NANOFIBROUS MEMBRANE FOR ASTHMA DETECTION

SUMMARY

In this study, a membrane consisting of zinc oxide nanofibers was formed through electrospinning process in order to be used in gas sensing tests for determining the nitrogen oxides (NO_x) gases which exist in the exhaled breath of asthma patients more than those of healthy people. Various attempts had been made to get the best result concerning the ease and continuity of the process at production step. Polyvinyl alcohol (PVA) and Zinc acetate dihydrate ($Zn(OAc)_2 \cdot 2H_2O$) were used as precursor substances for membrane formation. Zinc oxide (ZnO) nanofibers-based membranes were obtained after calcination process. In order to determine the best polymer concentration for electrospinning solutions; PVA solutions at concentrations ranging from 7% to 20% (w/v) were prepared, firstly. According to the rheological study results, 15% PVA (w/v) was found the most proper concentration among them in terms of the level of the polymer chain entanglement that provided sufficient viscosity. Four different mass ratio of $Zn(OAc)_2 \cdot 2H_2O$ with respect to the polymer concentration; 1:0.5, 1:1, 1:1.5 and 1:2 were introduced to the solutions for finding the most proper electrospinnable solution for ZnO formation. Some physicochemical and rheological analyzes such as pH, conductivity, viscosity and surface tension measurements were carried out in order to evaluate the electrospinnability of each solution and also to suggest the possible reactions of intermediate products formed in aqueous medium. The conductivity, surface tension and viscosity values of the solutions increased with an increase in $Zn(OAc)_2 \cdot 2H_2O$ concentration; however, a decrease in pH was observed. This was probably due to the consumption of the hydroxide ions in PVA / $Zn(OAc)_2 \cdot 2H_2O$ solutions, in order to form an aqueous intermediate product, zinc hydroxide $Zn(OH)_2$. Moreover, thermogravimetric analysis (TGA) was carried out for defining suitable thermal parameters for calcination process. The scanning electron microscopy (SEM) analysis was employed to the membranes prepared both before and after calcination processes. As far as the all analyzes and measurements were concerned, it was estimated that the formation of ZnO overlapped with the late decomposition of PVA during the thermal process, around 600°C. The formation of ZnO proceeded through the transformation of $Zn(OH)_2$ by loss of water molecule. Among the prepared samples, 15% PVA solution with equivalent amount of $Zn(OAc)_2 \cdot 2H_2O$ showed the best performance considering the fineness of nanofibers and the amount of products or reactants produced or used; however, the continuity and stability at the region of taylor cone and jet were not found satisfactory enough. That is the reason why, various attempts were applied to all samples in order to get more optimized electrospinning process. In the last part of the study, the solutions were re-prepared and investigated in acidic and basic medium, in water:ethanol binary solvent system and in the presence of surfactant. After conducting all necessary analyses, it was concluded that adding 1% (w/v) non-ionic surfactant to the solution of 15% PVA:

15% $Zn(OAc)_2 \cdot 2H_2O$ provided more stable and continuous electrospinnability predominantly thanks to the decrease in surface tension of the solution.

ASTIM HASTALIĞININ TAYİNİ İÇİN GAZ ALGILAYICI NANOLİFLİ MEMBRAN GELİŞTİRİLMESİ

ÖZET

Bu tez çalışmasında; sağlıklı insanlara kıyasla astım hastalarının nefeslerinde daha fazla miktarda bulunan azot oksit (NO_x) gazlarının tayininde kullanılmak üzere bir membran üretilmeye çalışılmıştır. Bilindiği üzere solunum sisteminin temel görevi canlı yaşamı için gerekli oksijeni sağlamak ve canlı bünyesindeki karbondioksiti dışarı atmaktır. Solunan havanın içerisinde bulunan oksijen, akciğerlerdeki alveoller vasıtasıyla kana difüze olur ve kan dolaşımı ile organlara, ve dolayısıyla hücrelere geçerek hücrelerin oksijen ihtiyacını karşılar. Buna eş zamanlı olarak; hücrelerde oluşan gaz haldeki metabolik atıklar da difüzyon ile kana geçer ve kan dolaşımı ile tekrar akciğerlere ulaşır, soluk verme ile dışarı atılırlar. Bu metabolik atıkların en bilineni karbondioksit olsa da verilen nefes içerisinde 3500'den fazla bileşen olduğu araştırmalar sonucunda bilinmektedir. Bu bileşenlerden başlıcaları azot, oksijen, su ve inert gazlar olmakla beraber konsantrasyonu trilyonda bir (ppt) ile milyonda bir (ppm) arasında değişen çok düşük miktarda uçucu organik bileşikler de yer almaktadırlar. Verilen nefeste yer alan bileşenlerden kimileri, bazı hastalıklarla ilişkilidirler ve bu nedenle hastaların nefesinde nicelik olarak sağlıklı insanlara kıyasla daha fazla bulunabilirler. Dolayısıyla, verilen solukta bulunan kimi bileşenler aynı zamanda ilgili hastalıkların nefes belirteçleri olarak da kabul edilmektedirler. Astım hastalığı özelinde ise bu nefes belirteci azotmonoksittir (veya nitrik oksit). Ancak kimyasal kararlılığı düşük bir molekül olduğundan ötürü, ortamdaki diğer türlerle olası reaksiyonlarını da göz önünde bulundurmak çoğu tayin yöntemlerinde dikkate alınması gereken bir husustur. Bu nedenle başvurulan tayin yöntemleriyle yapılan analizlerde tüm azot oksit türlerinin (NO_x) potansiyeli dikkate alınmalıdır. Nefes ile ilgili hastalıkların analizinde çeşitli yöntemler mevcuttur ve bu yöntemler temel çalışma prensiplerine göre üç ana grupta toplanabilirler: gaz kromatografisi veya kütle spektrometrisine dayalı yöntemler, lazer absorpsiyon spektroskopik yöntemleri ve kimyasal sensörler. Bahsedilen yöntemler arasında kemo-dirençli gaz sensörleri veya kısaca kemorsistörler, nefes analizlerinde sıkça tercih edilen uygulamalardandır. İçeriklerinde bulunan malzemeler, onları gaz algılama açısından işlevsel kılmaktadır. Algılayıcı sensör malzemesi olarak genellikle metal oksitler yaygın olarak yararlanılan malzemelerdir. Diğer yöntemlerle karşılaştırıldığında; metal oksit bazlı sensörler, daha küçük hacimli sistem ve düşük maliyetli üretim gibi çeşitli avantajlar sağlarlar. Spektroskopik ve kromatografik yöntemlere göre daha basit olmaları ve çalışma prensiplerinin karmaşık olmayışı onları rutin klinik testlerde cazip kılmaktadırlar. Bu çalışmada gaz sensörü uygulamalarında kullanılmak üzere bir membran üretilmeye çalışılmıştır. Çinko oksit nanoliflerinden oluşan söz konusu membran elektrospinning yöntemi ile elde edilmiştir. Devamlı ve kesintisiz bir üretim süreci için deneysel çalışmalar aşamasında çeşitli araştırmalara gidilmiştir. Polivinil alkol (PVA) ve çinko asetat tuzunun dihidratı ($Zn(OAc)_2 \cdot 2H_2O$) membran üretimi için öncü (prekürsör) maddeler olarak kullanılmışlardır. Hedef ürün olan çinko oksit (ZnO) nanoliflerinden

oluşan membran ise kalsinasyon işlemi sonrasında elde edilmiştir. Deneysel çalışmaların başlangıcında, en iyi performansı veren elektrospinning çözeltisini bulmak için konsantrasyonları %7 ile %20 (w/v) arasında değişen PVA sulu çözeltileri hazırlanmıştır. Bilindiği üzere başarılı bir elektrospinning işlemi için, işlem sırasında kullanılan çözeltinin belli bir viskoziteye sahip olması gerekir ve bu da ancak çözeltideki polimer zincirlerinin birbirlerine dolanma düzeyinin yeterli olması sonucunda sağlanabilir. Reolojik çalışmalara göre, hazırlanan çözeltiler arasından %15 (w/v) konsantrasyonundaki PVA çözeltisinin bu koşulu sağladığı görülmüştür. Diğer adımda, ZnO eldesi için prekürsör madde olan çinko asetat dihidrat tuzunun %15 (w/v) PVA içermesi kararlaştırılmış elektrospinning çözeltisindeki en uygun derişimini bulmak amacıyla ne kadar eklenmesi gerektiği araştırılmıştır. Bu bağlamda, kütle oranları polimer miktarına göre 1:0.5, 1:1, 1:1.5 ve 1:2 olan dört farklı konsantrasyonda $Zn(OAc)_2 \cdot 2H_2O$ çözeltileri hazırlanmıştır. Tuzun eklenmesiyle sulu ortamda oluşabilecek olası ara ürünlerin olası reaksiyonlarını kestirebilmek ve ayrıca her bir çözeltinin elektrospinlenebilirliğini yorumlayabilmek amacıyla; pH, iletkenlik, viskozite ve yüzey gerilimi testleri gibi bazı fizikokimyasal ve reolojik analizler yapılmıştır. Yapılan analiz sonuçlarına göre çözeltilerin iletkenlik, yüzey gerilimi ve viskozite değerleri artan $Zn(OAc)_2 \cdot 2H_2O$ konsantrasyonuna bağlı olarak artış gösterirken sadece pH değerlerinde düşüş gözlemlenmiştir. Bu düşüşün muhtemel nedeni; PVA / $Zn(OAc)_2 \cdot 2H_2O$ çözeltilerindeki hidroksit iyonlarının, bir sulu ortam ara ürünü olan çinko hidroksitin ($Zn(OH)_2$) oluşumu için tüketilmesidir. Kalsinasyon işleminde uygun termal parametrelerin bulunması için; hem sadece PVA içeren elektrospinlenmiş numuneye, hem de PVA / $Zn(OAc)_2 \cdot 2H_2O$ içeren elektrospinlenmiş numuneye termogravimetrik analizler (TGA) yapılmıştır. Kalsinasyon işleminden önce ve sonra elde edilen numune membranların topografyasını ve kompozisyonunu incelemek için SEM analizinden de faydalanışmıştır. Yapılan tüm analizler ve ölçümler dikkate alındığında; termal işlemde ZnO oluşumunun, PVA'nın geç dekompozisyonu ile 600°C civarında örtüştüğü tahmin edilmiştir. ZnO'nun oluşumu, $Zn(OH)_2$'nin bir su molekülü kaybı ile olan transformasyonu ile gerçekleşmiştir. Nanoliflerin inceliği ve giren/çıkan maddelerin miktarları, bir diğer deyişle verimleri göz önünde bulundurulduğunda; hazırlanan numuneler arasında eşdeğer miktarda $Zn(OAc)_2 \cdot 2H_2O$ ve PVA içeren çözelti en iyi performansı göstermiştir, ancak taylor konisi ve jet bölgesindeki süreklilik ve stabilite yeterince tatmin edici bulunmamıştır. Bu nedenle daha optimize bir elektrospinning prosesine erişmek için çeşitli girişimlerde bulunulmuştur. Yapılan çalışmaların son bölümünde numune çözeltiler; asidik ve bazik ortamlarda, su : etanol ikili solvent karışımlarında ve yüzey aktif madde (surfaktan) varlığında yeniden hazırlanarak tekrar incelenmişlerdir. Asidik ortam çalışmaları pH değerinin 3.5 civarında olduğu bölgede yapılmıştır. Her ne kadar çözelti homojenliği bakımından herhangi bir sorun gözlemlenmediyse de; asetik asit çözeltisinde hazırlanan %15 PVA : %15 $Zn(OAc)_2 \cdot 2H_2O$ çözeltisinin viskozite değerinin, sadece su kullanılarak hazırlanan çözeltinin viskozite değerine kıyasla %46.87 oranında fazla oluşundan dolayı bu seçenek ile ilerlenmemiştir. Hemen ardından yapılan bazik ortam çalışmaları da sonuçsuz kalmıştır. $Zn(OAc)_2 \cdot 2H_2O$ tuzunun sulu çözelti ortamında verdiği bir çözünme ürünü olan çinko hidroksitin, $Zn(OH)_2$, pH değerinin 8 ile 12 olduğu bölgede gösterdiği çok zayıf çözünebilirlik nedeniyle bazik ortam çalışmaları pH değerinin 8'in altında ve 12'nin üstünde olduğu bölgeler ile kısıtlanmıştır. pH değerinin 8'in altında olduğu bölge, mevcut numunenin pH değerine yakın bir bölge olduğundan, bu bölgede hazırlanan numunelerde dikkate alınır bir fark gözlemlenememiştir. pH değerinin 12'nin üzerinde olduğu bölgede de, muhtemelen PVA polimerindeki yan gruplar olan hidroksil gruplarının

deprotonlanması sonucu görülen viskozitedeki keskin düşüş nedeniyle elektrospinlenebilir bir çözelti elde edilememiştir. Bir diğer çalışmada ise çözücü olarak kullanılan distile su yerine distile su ve etanol ikili solvent sistemi kullanılmıştır. Karışımdaki etanol miktarına bağlı olarak görülen çözünme problemleri nedeniyle, etanol konsantrasyonunun %10 (v/v) ve %20 (v/v) olduğu iki numune incelenmiştir. Hazırlanan her iki numune her ne kadar homojen olsa da, organik çözücülerin doğası gereği gösterdikleri düşük iletkenlik nedeniyle hazırlanan numunelerin iletkenlik değerlerinde sırasıyla %38.84 ve %61.95 civarında düşüş gözlemlenmiştir. Ayrıca, etanol su karışı ile hazırlanan numunelerin viskozite değerlerinde de sırasıyla %14.91'lik ve %31.26'lik artışlar görülmüştür. Fakat, son çalışmada kullanılan surfaktan etkili sonuçlar vermiştir. Her ne kadar surfaktan miktarının görece yüksek olduğu değerlerde çözeltide çözünmemiş kısımlar gözlemlense de surfaktan miktarının düşük tutulduğu aralıkta homojen ancak renk olarak şeffaflığını kaybetmiş numuneler elde edilmiştir. Yüzey gerilimi testi dışında, %1 (w/v) oranında non-iyonik surfaktan içeren %15 PVA : %15 $Zn(OAc)_2 \cdot 2H_2O$ çözeltisine yapılan tüm fizikokimyasal analizlerin ve viskozite ölçümlerinin sonuçları surfaktan içermeyen numunenin sonuçları ile yüksek yakınlık göstermişlerdir. Muhtemelen yüzey geriliminde görülen %20'lik düşüş sayesinde, daha stabil ve sürekli elektrospinlenebilirlik sağlandığı sonucuna varılmıştır.

1. INTRODUCTION

1.1 Purpose of the Thesis

In this study, we aimed to produce a membrane consisting of zinc oxide nanofibers through electrospinning process in order to be used in gas sensing tests for determining the nitrogen oxides (NO_x) gases which exist in the exhaled breath of asthma patients more than those of healthy people. The experimental research work can be defined in following three main steps:

(1) Preparation of a solution with inorganic precursor (zinc acetate dihydrate) and polymer content (polyvinyl alcohol), and achieving the feasible viscosity for electrospinning by finding the appropriate mass ratio.

(2) Spinning of the electrospinning solution in order to obtain precursor nanofibers of polymer/inorganic composite.

(3) Calcinations of the precursor composite fibers in order to obtain final zinc oxide nanofibers.

In the hope of evaluating each step and making necessary improvements when required, several measurements and analyzes had been applied in experimental research. Some physicochemical analyzes such as pH, conductivity, viscosity and surface tension measurements were performed during the wet chemical processes. Except pH measurements, the primary purpose of the all tests were performed was defining optimized electrospinning conditions in terms of parameters; hereby, the reason of the possible deviation from optimized electrospinnability caused by any new attempts could be followed and readjustments could be applied. The pH investigations were made to follow the fate of the precursor zinc salt in the aqueous environment. The scanning electron microscopy (SEM) analysis was employed for monitoring the electrospun structures in both pre- and post- calcination processes. The thermogravimetric analysis (TGA) was carried out for defining proper thermal parameters for calcination.

Having evaluated the data derived from the first attempts, it was decided to make improvements on the solution step for obtaining better electrospinning performance. Therefore, the solutions were re-prepared and investigated in acidic and basic medium, in water:ethanol binary solvent system and in the presence of surfactant. In order to compare the results with those of previous attempts; pH, conductivity, viscosity and surface tension measurements were performed along with SEM and TGA to all newly prepared solutions.

The goal tree of the project, which describes the striking points of whole picture, can be found below in Figure 1.1. Considering the performance of the final product in terms of functionality and usability, the basic characteristics of the project has revealed after creating this general visualization. More specifically, however, this study aims to propose the formation reaction(s) of zinc oxide and to suggest related attempts for better electrospinnability in the light of these reactions.

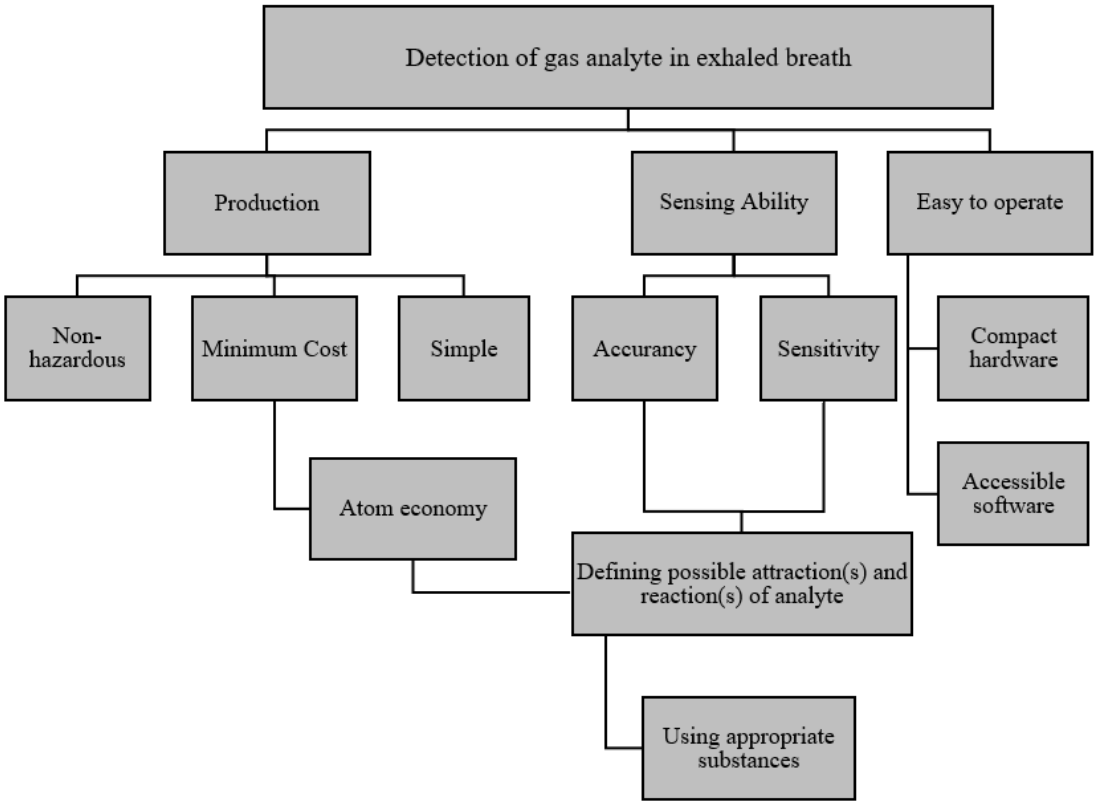

Figure 1.1 : The goal tree of the project.

1.2 Literature Review

The simultaneous journey of the medicine and technology from ancient to present times can be a great example for continuous growth; any progress in one has been accepted as a spark for ignition, and so has led to progress also the other [1,2,3]. Thanks to this cooperative evolution, the diagnosis of many diseases is made by highly reliable modern methods, equipment and devices. Among them, lab-analysis of bodily fluids such as blood and urine or tissue analysis are publicly popular and well-known methods; however, analysis of exhaled breath is another method utilized for clinical diagnosis commonly. It is a harmless and painless method for patients and may enable quick and non-invasive diagnosis of a certain number of illnesses, including cancer and diabetes [1,3].

As it is known, the oxygen need of the body is met through lung; inhaled oxygen diffuses from the alveoli to the blood and spreads throughout the body thanks to blood circulation. Meanwhile, the waste product of cellular metabolism, carbon dioxide (CO_2), leaves from the cells in order to be removed through exhaled breath [3,4]. However, not only the body get rid of CO_2 through breathing out, but also other gaseous metabolic wastes and species removes. It is known that more than 3500 different components have been found in exhaled breath, and still continually growing. The composition and concentration of exhaled breath is stated briefly in Table 1.1; which are mainly followings: nitrogen, oxygen, CO_2, water, inert gases, and very low amount of volatile organic compounds (VOCs) whose concentration varies between parts per trillion (ppt) to parts per million (ppm). Among the VOCs, some of them can be related with some diseases; and therefore, they can be found in the breath of patients quantitatively more than those of healthy people. That is the reason why, some VOCs exist in the exhaled breath are also accepted as breath markers. Specific diseases have specific breath markers. For example; the concentration of acetone is quite higher in the case of patients with uncontrolled diabetes. Another VOCs that can present in the breath, ammonia, is slightly higher who has kidney disease and/or bacterial production in a mouth [4].

The disorders of the respiratory system also show such markers. Many lung diseases; bronchiectasis, cystic fibrosis, and interstitial lung disease etc., and most commonly

known asthma and chronic obstructive pulmonary disease can be monitored through the breath markers [3,5]. Although new studies recently have focused on the possible

Table 1.1 : Some major and minor compounds and its concentrations for the breath of healthy people [2].

Compound in Breath	Concentration
Nitrogen	78.04%
Oxygen	16%
Carbon dioxide	4%–5%
Carbon monoxide	0–6 ppm
Ammonia	0.5 ppm–2 ppm
Acetone, Isoprene and Ethanol	0.9% <1 ppm
Hydrogen sulphide	0–1.3 ppm
Nitric oxide	10 ppb–50 ppb
Nitrous oxide	1 ppb–20 ppb
Ethane	0–10 ppb

volatile gases exist such as ethane and pentane for monitoring the pulmonary diseases, exhaled carbon monoxide and nitric oxide are the most extensively studied exhaled markers among them. Especially, nitric oxide (NO) is a well-known biomarker that is particularly associated with asthma, even it is not specific marker for this disease. The limits of the elevated levels of NO in the breath of asthmatics depend on many variables such as smoking addiction or any other disease that can promote the NO production; however, NO concentration that is greater than 50 ppb can supposably be accepted as a high level [5,6].

1.3 Methods for Breath Analysis

Although in this study the nitric oxide is emphasized in terms of its role in physiological and biological processes, it has also an importance in industrial and environmental sciences [7,8]. Therefore, common instrumental analysis techniques are used for detection and measurement of biomarkers exist in exhaled breath; especially spectroscopic and chromatographic methods. Gas chromatography, proton transfer reaction-mass spectrometry, selected ion flow tube-mass spectrometry, laser photoacoustic spectroscopy, differential mobility spectrometer, colorimetric sensor arrays, chemiluminescence analyzer, colorimetric sensor arrays and nanomaterials for breath gas analysis are some techniques for breath gas analysis [2]. These techniques can be used either alone or sometimes integrated with each other to increase the

sensitivity and/or detection limit. All the methods aforementioned one by one can be categorized into three groups according to their principle behind: methods based on gas chromatography or mass spectrometry (single or integrated), laser-absorption spectroscopic methods and chemical sensors (including arrays) [2,3].

1.3.1 Chemosensory measurement for breath diagnosis: chemosensors as nanomaterials for breath gas analysis

Among the mentioned concepts, chemo-resistive gas sensors, or shortly chemorsistors, are most commonly preferred application for breath detection. The material that chemosensors are made render them functional in terms of gas sensing, and generally metal oxides are extensively benefited element for sensing technology. In comparison to other methods, chemo-resistors based on metal oxides provide several advantages such as great potential of downsizing and low-cost manufacture. They are simple compared to spectroscopic and chromatographic methods; the working principle is not complicated; that is the reason why, they can be miniaturized thanks to the developments in nanoscience. They are cheap since they are simple compared to other instrumental analysis devices, make them attractive for routine clinical tests [3,9].

The gas sensing ability of chemosensors is based on the electrical properties of the material that are made by, mostly metal oxide semiconductor. When the target gas is applied to the metal oxide semiconductor, it will make a change on electrical resistance of the gas sensing element depending on the oxidizing or reducing character of the target gas. This change can be followed by measuring the electrical resistance of the semiconductor material during the test. The time for exposure, the physical and chemical characteristics of the exposed gas compound and the semiconductor can be cited some dependent variables that have direct effects on the analyzes [3,9].

1.3.2 The sensing mechanism of metal oxides and NO_x as a target gas

The working mechanism of the chemo-resistive gas sensors, in which metal oxides are used as a sensing element, can be explained through the concept of receptor and transducer functions; since they sort of constitute chemical sensors [9]. The term receptor function is related to the chemical substance that will be analyzed or identified, and the transducer function is related to the sensing element; which generates the response signal that is derived after the differential of two functions. The following illustration will be more explanatory to explain the sensing phenomenon.

The surface of the metal oxides is active side of the sensing mechanism of surface sensitive resistor sensors as their surface are susceptible to adsorption of the oxygen molecules in the presence of the air especially in the dry medium. Since the adsorption of the substance, oxygen, is occurred through chemical bond formation instead of physical attractions; the process is also called chemisorption of the oxygen ion. The chemisorption of the ions also can be defined as ionosorption [10]. Having defined all concepts, it is possible to be concluded that the surface layer of the surface sensitive resistor sensors ionosorbs the charged oxygen species as illustrated in Figure 1.2 (a).

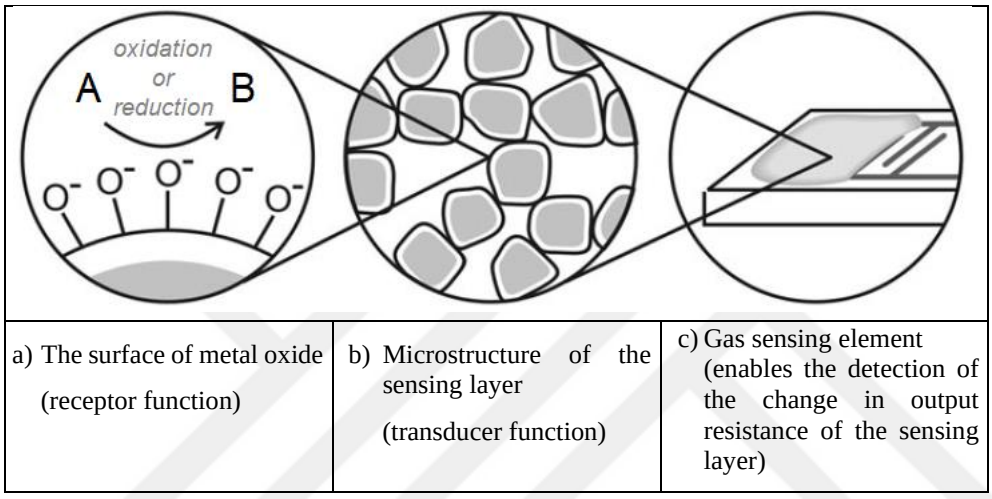

a) The surface of metal oxide (receptor function)	b) Microstructure of the sensing layer (transducer function)	c) Gas sensing element (enables the detection of the change in output resistance of the sensing layer)

Figure 1.2 : Schematic view of the surface of a semiconductor gas sensor (adapted from Ref. [9]).

The type of the ionosorbed charged oxygen species can vary depending on the operating temperature [9,11]. The exposed target gas is recognized by the metal oxide surface through gas-solid interaction or gas-solid reaction at operating temperature. This exposure leads to an electronic change of the metal oxide surface, in other words, receptor function. However, this change is not limited with the surface; electronic process continues by the role of bulk. Depending on the adsorbed species, electron transfer occurs from the surface chemical species to the bulk, or vice versa, from the bulk to the surface; which cause a change in the transducer function, or in other words, the resistance of the sensoring material. Thus, the resistance either decreases or increases as a result of the parameters that affect. For instance; in the case of n-type semiconductors, the exposure of reducing gases (such as H_2, CO, H_2S, NO) cause an increase in conductivity; however, the exposure of the oxidizing gases (such as NO_2, O_3, N_2O) have opposite effect on conductivity, it decreases. Another opposition can

be seen in p-type semiconductors. The exposure of reducing gases lead to a decrease in the conductivity, whereas the effect of oxidizing gases is vice versa [12].

Up to now, the changes and shifts between receptor and transducer were explained; however, the target analyte, which is the initiating factor of whole mechanism, also should be denoted. Figure 1.2 (a) is not only the illustration for the chemisorbed charged oxygen species and the surface, but it also explains the states of target analyte both pre- and post- exposure through labels of "A" and "B", respectively. To be given an idea, it could be supposed that the target analyte "A" would be carbon monoxide (CO) gas. The CO would be oxidized to carbon dioxide (CO_2), referred as label "B", as far as it interacts with the metal oxide surface because the necessity is supplied by chemisorbed oxygen species at the surface [9,12]. The same phenomenon can be seen also as the target gas is H_2, oxidation of H_2 to H_2O [12]. It is possible to explore the solid-state gas detecting mechanism through other examples, as well as NO. However, the stability of the target analyte should be taken into consideration when exposed gas is NO since it is unstable with respect to previous examples; and therefore, it is very sensitive to environmental conditions. According to the compounds present in the medium, other species that contain nitrogen and oxygen can be formed [8]; some of them might be followings:

$$NO + O_2 \longrightarrow NO_3 \qquad \text{reaction (1)}$$

$$NO + NO_3 \longrightarrow 2NO_2 \qquad \text{reaction (2)}$$

$$NO + NO_2 \longrightarrow N_2O_3 \qquad \text{reaction (3)}$$

That is the reason why; not only NO, but the family of oxide nitrogen species (NO, NO_2, N_2O, etc.), specifically nitric oxides (NO_X), are generally studied in the gas sensing investigations [2,7,8].

1.3.3 The nanostructures of a zinc oxide as a sensing material

As mentioned in previous section, the form of nanomaterial of metal oxides are widely used in gas-sensing applications. Titanium dioxide (TiO_2), tin dioxide (SnO_2) and tungsten trioxide (WO_3) are commonly used metal oxides, which are frequently seen for sensing acetone, ethanol and hydrogen sulfide, respectively. In order to increase the sensitivity of sensing; it is possible to see in some applications in which one of

them is used as a doping agent for the other [3]. However, another metal oxide, zinc oxide (ZnO), is a more commonly seen metal oxide in this field. The unique physical and chemical properties of ZnO such as perfect chemical stability, high efficiency between electrical and acoustic energy, broad range of radiation absorption and photostability render this material multifunctional. Additionally; its low toxicity, biocompatibility and biodegradability make it perfect candidate to be used in biomaterial industry [13].

1.3.3.1 Manufacture of ZnO nanofibers: from early process "aqueous solution" to further step "calcination"

Zinc oxide nanomaterials can be produced by various methods depending on the role in final product. Those methods based on physical or chemical processes, which are sol–gel, precipitation and co-precipitation, chemical vapour deposition, microwave-assisted technique, hydrothermal, solvothermal and magnetic sputtering can be cited as some examples for production of ZnO nanomaterials [14,15]. Each method has its own advantages and disadvantages, but the determining factor for the choice of methodology is usually the dimension and morphology of the nanomaterial. Nanospheres, nanorods, nanotubes, nanoplates, etc. can be obtained thanks to different procedures; for example, nanowires can be obtained through hydrothermal method, but chemical precipitation is generally applied in the case of nanotubes [15]. As mentioned in previous sections, the adsorption of the species and the analytes to the surface of metal oxide semiconductor is very crucial for gas sensoring measurements. That is why, the nano-structure of the ZnO gas sensing material should have as much surface area-to-volume ratio as possible in order to have better adsorption ability. Among the nanostructures, nanofibers would be proper structure owing to high porosity and surface area-to-volume ratio [16].

The route for synthesis of the ZnO nanofibers is determined according to the method selected. In this project, the synthesis journey of ZnO begins with wet chemical processes and ends in thermal treatment. The electrospinning method was used for nanofiber production; however, the details of the electrospinning technique will be explained in detailed in section 1.4. In short; among the many parameters that must be taken into consideration during the electrospinning process, the rheological behavior of the liquid that pumped into the system has importance in sample preparation stage.

Predominantly, this liquid is either the molten state of the target material (generally polymer) or its solution in a proper solvent [16]. In general, metal oxide nanofiber production benefited from the polymers which are a kind of template /or carrier polymer in the whole procedure. Especially, they provide perfect dispersion environment for newly formed inorganic sol species in prepared solution in the matter of target metal oxide material is not used directly in the electrospinning solution. Certainly, the contribution of the presence of polymers with high enough molecular weight in the solution to the rheological properties should also be noted as the relationship between molar mass and viscosity is concerned [16].

In the cases in which ZnO is not used directly in the solutions, the synthesis can be achieved through sol-gel method by using inorganic precursors, especially related metal salts. Therefore, many zinc-containing metal salts and synthesis paths can be suggested through different chemical reactions. Zinc chloride ($ZnCl_2$), zinc nitrate ($Zn(NO_3)_2$), zinc sulphate ($ZnSO_4$) and zinc acetate ($Zn(CH_3COO)_2$ or $Zn(OAc)_2$) can be cited as the examples of precursor zinc metal salts [13]. Each precursor leads to obtain zinc oxide; but in different solvents or environments, with different chemical reagents; and accordingly, through different chemical reactions. For instance, zinc chloride is generally used as a precursor salt in mechanochemical processes, which contain milling and heating processes. The powder form of precursor salt zinc chloride reacts with another regular inorganic salt in a ball mill to give intermediate product, $ZnCO_3$, whose thermal decomposition product will be ZnO [13].

$$ZnCl_2 + Na_2CO_3 \longrightarrow ZnCO_3 + 2NaCl \qquad \text{reaction (4)}$$

$$ZnCO_3 \xrightarrow{\Delta} ZnO + CO_2 \qquad \text{reaction (5)}$$

Such examples can be given more. In wet chemical process, ZnO can be obtained by using zinc acetate through sol-gel method. By adjusting the pH, ZnO formation can be seen in aqueous medium through following suggested reactions [15]:

$$Zn^{2+} + 2OH^- \longleftrightarrow Zn(OH)_2 \qquad \text{reaction (6)}$$

$$Zn(OH)_2 + 2OH^- \longleftrightarrow [Zn(OH)_4]^{2-} \qquad \text{reaction (7)}$$

$$[Zn(OH)_4]^{2-} \longleftrightarrow ZnO_2^{2-} + 2H_2O \qquad \text{reaction (8)}$$

$$ZnO_2^{2-} + H_2O \longleftrightarrow ZnO + 2OH^- \qquad \text{reaction (9)}$$

The source of the Zn^{2+} ions in aqueous medium is the zinc-containing metal salt; therefore, the concentration of Zn^{2+} ions in the medium directly depends on the salt amount. However, the fate of the zinc derivatives that may formed is not only related with zinc ion concentration; but also the amount of base added. The region in which pH is higher than 7, the first intermediate product, zinc hydroxide ($Zn(OH)_2$), can be observed as a result of reaction (6). However; further reactions or formations are possible. Another intermediate product, tetrahydroxozincate ion ($[Zn(OH)_4]^{2-}$), also can be formed at the saturated level of the zinc ions and especially hydroxide ions. The second intermediate product is a crucial reagent for formation of the final product, ZnO, through the possible reactions (8) and (9) [15]. It should be stated that, in order to proceed beyond the reaction (6); besides the saturated concentration, the temperature of the solution is also important. The formation of zinc hydroxide may not require as much heat as zinc oxide; the basic solution at 40 °C may lead to formation of $Zn(OH)_2$, but ZnO can be observed in aqueous solution at elevated temperatures, around 80 °C [17].

However, the formation of ZnO is not limited with abovementioned procedures. By using an organic template fiber, the precursor of inorganic material can be deposited on template surface; and after, the target material can be obtained through thermal treatments. Since organic materials are susceptible to decompose under heat, only inorganic species will remain after the decomposition temperature of selected organic matter [18,19]. If the previously mentioned $Zn(OH)_2$ is considered as the precursor inorganic material for zinc species, ZnO can be formed by the following reaction [19]:

$$Zn(OH)_2 \xrightarrow{\Delta} ZnO + H_2O \qquad \text{reaction(10)}$$

1.4 Literature Review for Electrospinning

Nanofibers belong to the category of one-dimensional (1D) structured materials, just as nanorods, nanotubes and nanowires; and offers many advantages thanks to their high specific surface area and particular enhanced chemical and physical properties that derives from their nano-level size [16,20,22]. Those properties differ from the bulk material because of the potential for quantum effects at the nanoscale. Additionally, the high surface area led to smaller particles to have more atoms on their surface, which allows them to respond more quickly to actions [21,22].

One-dimensional structured materials can be obtained in nanoscale through following methods and techniques: Electrospinning, self-assembly, phase separation, template synthesis, centrifugal spinning, etc. These methods can be classified according to the physical, chemical and biological perspectives, as well as they can be classified as spinning and non-spinning methods [22]. Among them, electrospinning has more advantages than others due to its flexibility of obtaining nanofibers by using a wide range of materials, ability to follow nanofiber diameter as well as morphology and fibrous structure and ease of adjustment the electrospinning solution by adding various soluble substances or nanomaterials. More or less, all kind of polymers can be electrospun in order to make nanofibrous constructions. They can be processed through by melting the polymer or dissolving the polymer in proper solvents. The diameter of the fibers can be adjusted during the process; by changing the parameters regarding the production, material or ambient condition, it is possible to increase or decrease the fiber diameter. Morphology is related with the surface in micro-structure scale. It can be modified by introducing several pores or changing pore characteristics. It is possible to change the fiber orientation by the way of distribution; one way or randomly distributed fibers. In order to achieve desired features, al kind of additives into the electrospinning solution can be added. For example, some nanometallic materials can be added to the solution in order to produce conductive material at the end. It is not important whether these additives are soluble or insoluble in the solution as long as appropriate process optimizations are made. The technique is not so expensive since high amount of material is not consumed. It is very simple technique with simple principles; establishment is not too complicated and huge. Ultimately, it is relatively robust and simple technique to produce nanofibers from a wide variety of polymers [16,20,23,24,25,26].

There are three main components in electrospinning set-up: power supply, pump that connected to the syringe and the collector. The necessary voltage is applied to syringe, so the solution at the tip of the needle is charged. Meanwhile, opposite or neutral charge is introduced at the collector in order to get charge difference between the syringe tip and the collector. The instability between these two charges let the electrospinning solution to move across to the collector by doing some movement, and accumulated on the collector. The dimensional formation of the material from tip of the needle to the collector can be in microscale or nanoscale; however, in both situation

molecular chains are becoming oriented in the direction of the collector, just as drawing effect. The drawing occurs in micro or nano level by applied electrical force. If a solvent is used to dissolve the polymer or any other additive; it is expected that the solvent should evaporate during this action and dry solid fibers are supposed to be accumulated on the collector at the end. Otherwise, the solvent remaining in the fibers collected at the collector can keep on dissolving the fibers again. That's why, optimizing parameters such as needle to collector distance, feeding rate and applied voltage are really important to get successful nanofibers [22,23,27,28].

1.4.1 Electrospinning parameters

All the efforts spent during electrospinning is for formation of fibrous structure without beads or any other defects. In order to achieve successful operation, many parameters must be balanced and compatible with each other. The electrospinning parameters are categorized into three sub-categories: solution parameters, production parameters and ambient parameters [29].

1.4.1.1 Solution parameters

Solution parameters are perhaps the most important among all because of its strong and directly effect on the result. The interaction between the selected polymers or materials with each other and/or the interaction of the selected polymers or materials with the selected solvent or solvent system are the factors that directly affect the properties of the solution such as viscosity, conductivity and surface tension. These parameters can be accepted as the dominant parameters in a regular electrospinning process. If there is a major problem or defect seen in a process due to the parameters mentioned, changes in ambient and production parameters may be insufficient; designing solutions or melts with different substances probably will be the proper way to solve the problem [29,30].

As it mentioned before, polymer melt or its solution can be used in electrospinning and the viscosity of it has influence on operation. Since the viscosity is the result of the interaction between all species in the medium, it is directly dependent on the molecular weight of the polymer, the concentration of the polymer in solution, any other solutes or impurities in the medium and ambient temperature. The interaction between species can increase or decrease depending on the level of aforementioned factors. If there are longer polymer chains in the medium due to the higher molecular

weight or more polymer chains due to the higher concentration, the viscosity increases as a result of the increased interaction between them; and vice versa. High viscosity levels may cause problems in feeding at the syringe pump system as well as increase in the requirement of power supply. In the case of low viscosity levels, dropping at the tip of the needle and the formation of beads along the newly formed fibers are commonly seen problems during the process. It is thought that irregularities in the distribution of the polymer in the solution may be the reason of the beads forming at low viscosity values [29,30,31,32].

Another important solution parameter is the conductivity of the solution or melt, which is the most important helping element to the electric force applied between the needle and collector; conductive samples are prone to be more charged. If a polymer solution or melt is not conductive enough, fibers may not form. The conductivity arises from the nature of the polymer and the solvent, the concentration of the electrospinning solution and the impurities or the additives in the solution such as salts. Sufficient amount of charged species carried from the needle to collector led to the obtainment of bead-free and fine fibers obtainment [29,31,33].

The electric field applied during the electrospinning is for basically overcoming the surface tension of the electrospinning solution in order to form jet. Thus, the level of the surface tension has another importance as a solution parameter. In cases in which the surface tension is high, the solvent used in solution can be changed since the surface tension is strongly dependent to the solution or solution systems; the addition of the surfactant can be another option for reducing it. High surface tension leads to the bead formation in fibers [29,31].

1.4.1.2 Production parameters

The strength of applied electrical field, feed rate or flow rate of the pump and the distance between needle tip to collector can be cited as main parameters for electrospinning methodology [30].

As mentioned previously, the surface tension should be overcome by applied voltage. Having reached this threshold, the droplet of the solution will lose its shape and form taylor cone at the tip of the needle thanks to this distortion. The shape and the length of the taylor cone, newly formed jet and the action of the fibers along the distance are directly related with the applied electrical power. Successful fiber production can be

achieved through the proper maturity of each stage. High voltage values cause longer jet formation, which limits the action of the species between the tip to collector; and therefore, can cause obtainment of relatively thicker fibers or electrospraying to the collector. In the contrary case, lower voltage values cause shorter jet formation and the species will spend more time for action between the distance tip to collector; which may cause the problem of not reaching the collector of newly formed fibers. However; in both two cases mentioned, the distance parameter was not taken into account. The optimum condition can be set also by changing the distance between the tip of the needle to collector; which is another process parameter. The morphology of the fibers also related with the distance because the solvent of the solution is evaporated and accordingly polymeric solution become solid during the travel distance. Unless polymeric material is not solidified, increasing the tip to collector distance will introduce more time for thinning to be occurred; and therefore, the diameters of the nanofibers will be decreased [29,30].

The element that feeds all mentioned parameters should not be forgotten, the feed rate or flow rate of the syringe pump. Feeding, in other words, the formation of the charged species, should be continuous. Otherwise; dropping at the tip of the needle is seen in the case of higher rates, and discontinuous electrospun fibers are collected in the case of lower rates. Thus, proper flow rate should be determined considering the mentioned electrospinning parameters, along with the spatial arrangement of the syringe such as vertical or horizontal [29,30].

1.4.1.3 Ambient parameters

The main ambient parameters, relative humidity and the temperature, are the parameters that independent from the personal preference. They can change on a day to day and place to place basis. They can affect the rate of solvent evaporation. Especially, the evaporation of the aqueous solutions in electrospinning process is adversely affected in humid environments. It can be seen also in non-aqueous solution; however, a different problem can also be observed in that case, the absorption of water by the solution during travel action. The negative effects of the humidity can be managed through a ventilation system [27,29,30]. The temperature parameter has another effect in addition to the evaporation rate. It can change the viscosity; as it increases, viscosity decreases [27,29,30].

2. MATERIALS & METHOD

2.1 Experimental Flow Diagram

Each step of the experimental work, in which all prepared and selected solutions were defined, could be seen below in Figure 2.1.

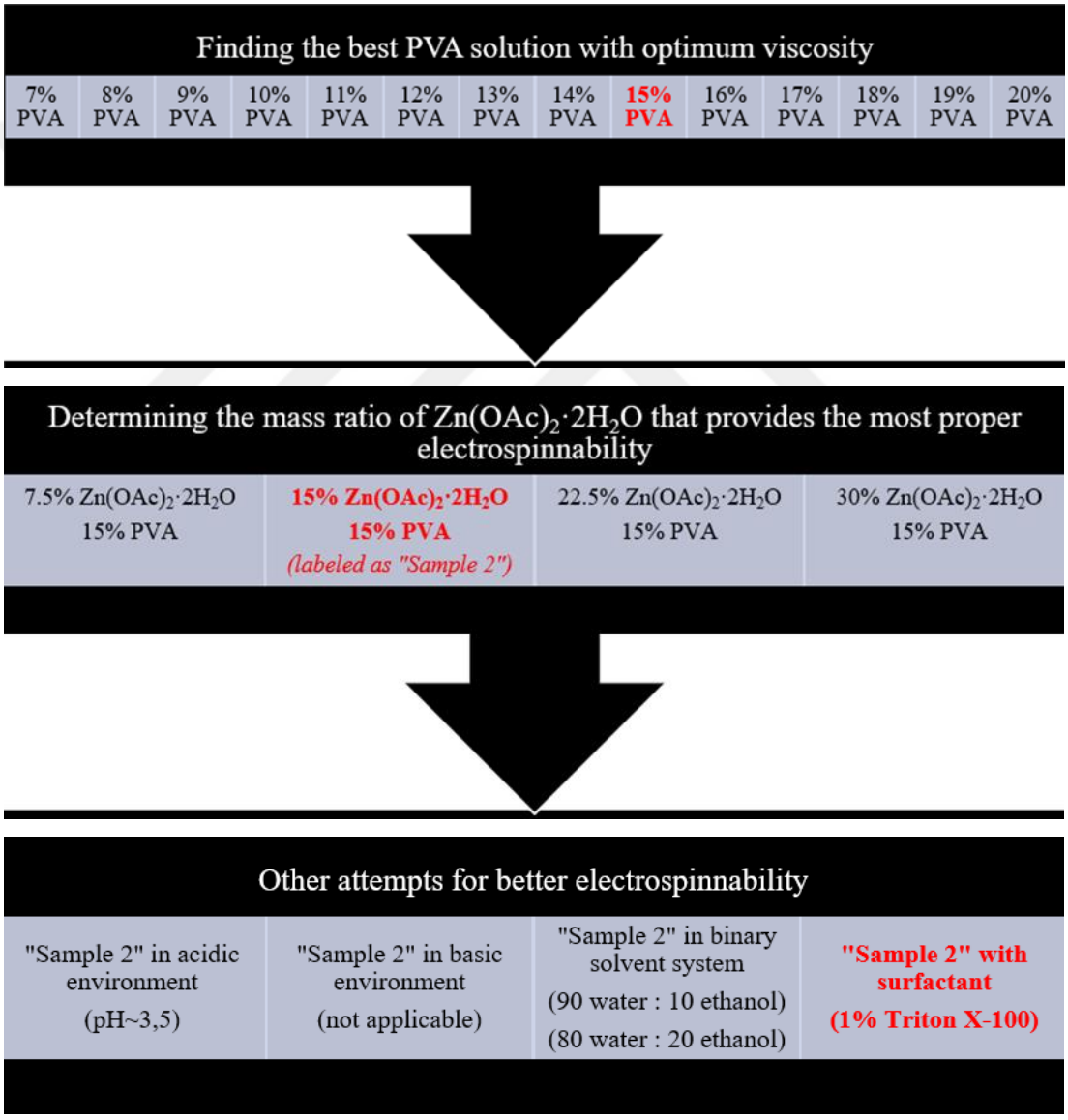

Figure 2.1 : The experimental flow diagram of the study.

2.2 Materials

Poly(vinyl alcohol), M_w 89,000-98,000, 99+% hydrolyzed, Zinc acetate dihydrate, ACS reagent, ≥98% were purchased from Sigma-Aldrich. Triton X-100 was purchased from Fluka. Ethanol absolute anhydrous was purchased from CARLO ERBA Reagents SAS. Acetic Acid 80% (Acide Acétique 80%) and Sodium Hydroxide 30% (Lessive de Soude 30%) solutions were purchased from Mon Droguiste.

2.3 Preparation of Solutions

The solutions prepared for each step were described in following sections.

2.3.1 Preparation of polyvinyl alcohol (PVA) solutions

The aqueous solutions of PVA in various concentrations were prepared in heating bath at 80 °C and stirred by magnetic stirrer for 2 h for complete solubilization of the polymer. PVA solutions were prepared by mixing the required amount of PVA and 10 mL of distilled water in relevant proportions (7%, 8%, 9%, 10%, 11%, 12%, 13%, 14%, 15%, 16%, 17%, 18%, 19% and 20% (w/v)). Having removed the hot polymer solutions from the heating bath, they were cooled to room temperature with constant stirring.

2.3.2 Preparation of PVA - zinc acetate dihydrate solutions

In this project, the zinc acetate dihydrate ($Zn(OAc)_2 \cdot 2H_2O$) was used as a precursor inorganic salt with the aim of obtaining zinc oxide (ZnO) nanofibers.

Four zinc acetate dihydrate solutions were prepared with different concentrations; 7.5%, 15%, 22.5%, 30% (w/v), by dissolving $Zn(OAc)_2 \cdot 2H_2O$ in 10 mL of distilled water. Ultrasonication was applied to promote an effective and fast dissolution of solid particles. The pH and conductivity measurements of each sample were done before adding the polymer. Then, 1.5 g of PVA was added to each solution in order to achieve the following mass ratios of PVA: $Zn(OAc)_2 \cdot 2H_2O$; 1:0.5, 1:1, 1:1.5 and 1:2. These samples were put in heating bath at 80 °C and stirred by magnetic stirrer for 2 h for complete solubilization of the polymer. Depending on the dissolution rate of the PVA, the fluidity of the solution was changed during this 2 h. Therefore, the speed of the magnetic stirrer should be checked at certain time intervals. Having removed the hot samples from the heating bath, they were cooled to room temperature with constant

stirring at proper level. The pH and conductivity measurements of each sample were done again for getting final results. The flow chart of the above-mentioned experiment is stated below in Figure 2.2.

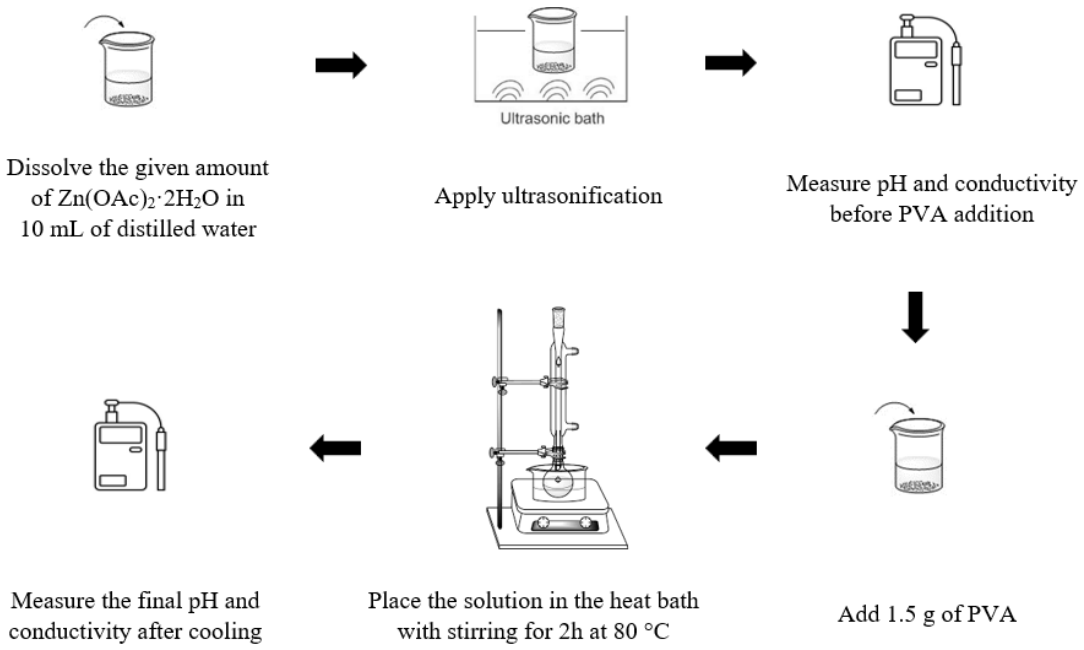

Figure 2.2 : The flow chart of PVA - zinc acetate dihydrate solution preparation.

The prepared samples that vary with respect to zinc acetate dihydrate concentration were stated in Table 2.1.

Table 2.1 : The label of the samples and corresponding concentration values.

Sample Label	PVA Concentration	$Zn(OAc)_2 \cdot 2H_2O$ Concentration	Mass Ratio of PVA: $Zn(OAc)_2 \cdot 2H_2O$
Sample 1	15% (w/v)	7.5% (w/v)	1:0.5
Sample 2	15% (w/v)	15% (w/v)	1:1
Sample 3	15% (w/v)	22.5% (w/v)	1:1.5
Sample 4	15% (w/v)	30% (w/v)	1:2

2.3.3 Preparation of PVA-zinc acetate dihydrate solutions in acidic medium

Four zinc acetate dihydrate solutions were prepared with different concentrations; 7.5%, 15%, 22.5%, 30% (w/v), by dissolving $Zn(OAc)_2 \cdot 2H_2O$ in 10 mL of 4M acetic acid solution. Ultrasonication was applied to promote an effective and fast dissolution of solid particles. The pH and conductivity measurements of each sample were done before adding the polymer. Then, 1.5 g of PVA was added to each solution in order to

achieve the following mass ratios of PVA: $Zn(OAc)_2 \cdot 2H_2O$; 1:0.5, 1:1, 1:1.5 and 1:2. These samples were put in heating bath at 80 °C and stirred by magnetic stirrer for 2 h for complete solubilization of the polymer. Depending on the dissolution rate of the PVA, the fluidity of the solution was changed during this 2 h. Therefore, the speed of the magnetic stirrer should be checked at certain time intervals. Having removed the hot samples from the heating bath, they were cooled to room temperature with constant stirring at proper level. The pH and conductivity measurements of each sample were done again for getting final results. The flow chart of the above-mentioned experiment is stated below in Figure 2.3. The prepared samples that vary with respect to zinc acetate dihydrate concentration were stated in Table 2.2.

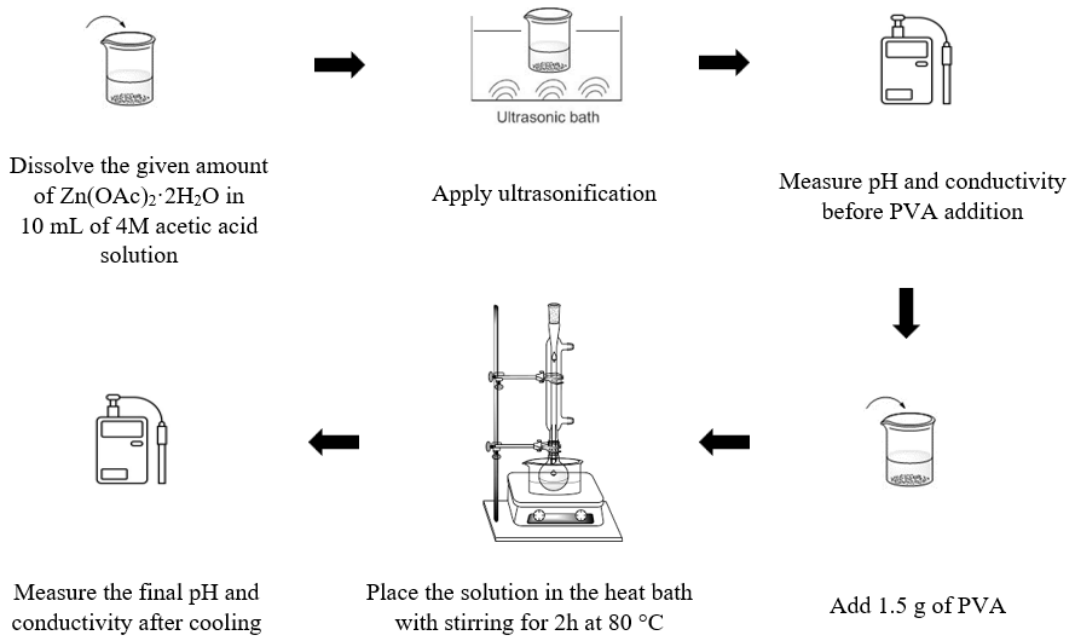

Figure 2.3 : The flow chart of PVA - zinc acetate dihydrate solution preparation in acidic medium.

Table 2.2 : The label of the samples and corresponding concentration values for acidic medium.

Sample Label	**PVA Concentration**	**$Zn(OAc)_2 \cdot 2H_2O$ Concentration**	**Mass Ratio of PVA: $Zn(OAc)_2 \cdot 2H_2O$**
Sample 1(Ac)	15% (w/v)	7.5% (w/v)	1:0.5
Sample 2(Ac)	15% (w/v)	15% (w/v)	1:1
Sample 3(Ac)	15% (w/v)	22.5% (w/v)	1:1.5
Sample 4(Ac)	15% (w/v)	30% (w/v)	1:2

2.3.4 Preparation of PVA-zinc acetate dihydrate solutions in ethanol/water binary solvent system

In this part of the study, two different concentrations of ethanol-distilled water mixture were used: ethanol: water (10:90) and ethanol: water (20:80). The flow chart of the below-mentioned experiments is stated in Figure 2.4. For each solvent system, four zinc acetate dihydrate solutions were prepared at different concentrations; 7.5%, 15%, 22.5%, 30% (w/v), by dissolving $Zn(OAc)_2 \cdot 2H_2O$ in 10 mL of ethanol: water mixture. Ultrasonication was applied to promote an effective and fast dissolution of solid particles. The pH and conductivity measurements of each sample were done before adding the polymer. Then, 1.5 g of PVA was added to each solution in order to achieve the following mass ratios of PVA: $Zn(OAc)_2 \cdot 2H_2O$; 1:0.5, 1:1, 1:1.5 and 1:2. These samples were put in heating bath at 80 °C and stirred by magnetic stirrer for 2 h for complete solubilization of the polymer. Depending on the dissolution rate of the PVA, the fluidity of the solution was changed during this 2 h. Therefore, the speed of the magnetic stirrer should be checked at certain time intervals. Having removed the hot samples from the heating bath, they were cooled to room temperature with constant stirring at proper level. The pH and conductivity measurements of each sample were done again for getting final results. The flow chart of the above-mentioned experiment is stated below in Figure 2.4.

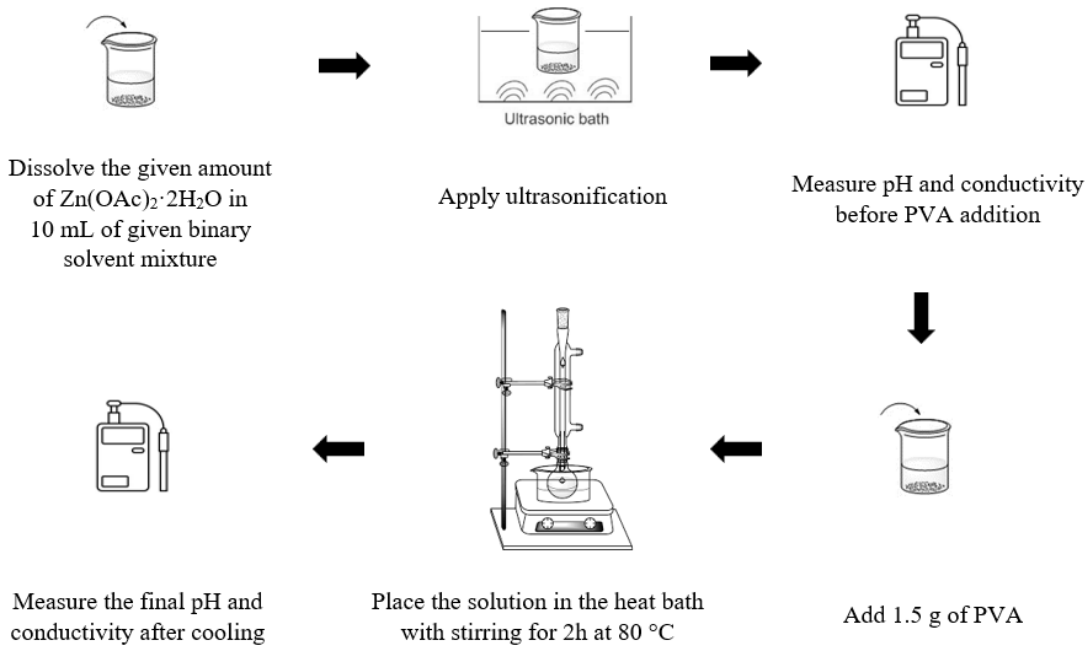

Figure 2.4 : The flow chart of PVA - zinc acetate dihydrate solution preparation in binary solvent system.

The prepared samples that vary with respect to the zinc acetate dihydrate concentration were stated in Table 2.3 and Table 2.4.

Table 2.3 : The label of the samples and corresponding concentration values for binary solvent system "ethanol:distilled water (10:90)".

Sample Label	PVA Concentration	$Zn(OAc)_2 \cdot 2H_2O$ Concentration	Mass Ratio of PVA: $Zn(OAc)_2 \cdot 2H_2O$
Sample 1(Eth10)	15% (w/v)	7.5% (w/v)	1:0.5
Sample 2(Eth10)	15% (w/v)	15% (w/v)	1:1
Sample 3(Eth10)	15% (w/v)	22.5% (w/v)	1:1.5
Sample 4(Eth10)	15% (w/v)	30% (w/v)	1:2

Table 2.4 : The label of the samples and corresponding concentration values for binary solvent system "ethanol:distilled water (20:80)".

Sample Label	PVA Concentration	$Zn(OAc)_2 \cdot 2H_2O$ Concentration	Mass Ratio of PVA: $Zn(OAc)_2 \cdot 2H_2O$
Sample 1(Eth20)	15% (w/v)	7.5% (w/v)	1:0.5
Sample 2(Eth20)	15% (w/v)	15% (w/v)	1:1
Sample 3(Eth20)	15% (w/v)	22.5% (w/v)	1:1.5
Sample 4(Eth20)	15% (w/v)	30% (w/v)	1:2

2.3.5 Preparation of PVA-zinc acetate dihydrate solutions containing surfactant

Four zinc acetate dihydrate solutions were prepared at different concentrations; 7.5%, 15%, 22.5%, 30% (w/v), by dissolving $Zn(OAc)_2 \cdot 2H_2O$ in 10 mL of distilled water. Ultrasonication was applied to promote an effective and fast dissolution of solid particles. In order to introduce 1% (w/v) concentration of surfactant to the solution, 0.1 g of Triton X-100 was added to each solution and stirred for a while to get homogeneous solution. The color change might be observed in the solutions after the addition of surfactant. If the color of the solution had changed from transparent to blurry, the solution had to be carefully examined in order to be ensured for the homogeneity. The pH and conductivity measurements of each sample were done before adding the polymer. Then, 1.5 g of PVA was added to each solution in order to achieve the following mass ratios of PVA: $Zn(OAc)_2 \cdot 2H_2O$; 1:0.5, 1:1, 1:1.5 and 1:2. These samples were put in heating bath at 80°C and stirred by magnetic stirrer for 2 h for complete solubilization of the polymer. Depending on the dissolution rate of the

PVA, the fluidity of the solution was changed during this 2 h. Therefore, the speed of the magnetic stirrer should be checked at certain time intervals. Having removed the hot samples from the heating bath, they were cooled to room temperature with constant stirring at proper level. The pH and conductivity measurements of each sample were done again for getting final results. The flow chart of the above-mentioned experiment is stated below in Figure 2.5.

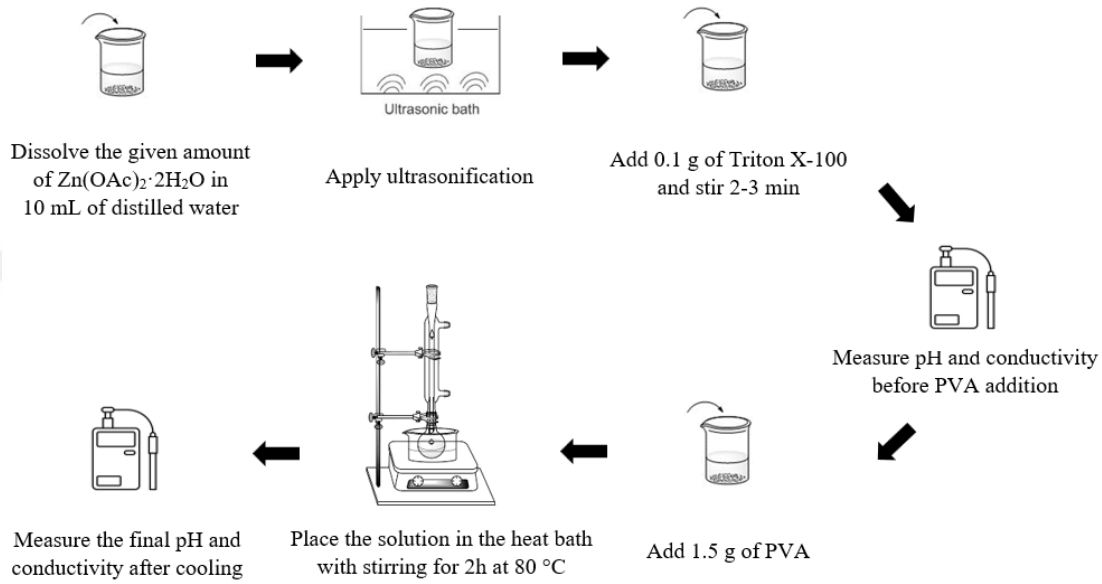

Figure 2.5 : The flow chart of surfactant containing PVA - zinc acetate dihydrate solution preparation

The prepared samples that vary with respect to zinc acetate dihydrate concentration were stated in Table 2.5.

Table 2.5 : The label of the samples and corresponding concentration values for surfactant solutions; 1% (w/v) of Triton X-100.

Sample Label	**PVA Concentration**	**$Zn(OAc)_2 \cdot 2H_2O$ Concentration**	**Mass Ratio of PVA: $Zn(OAc)_2 \cdot 2H_2O$**
Sample 1(TrX1)	15% (w/v)	7.5% (w/v)	1:0.5
Sample 2(TrX1)	15% (w/v)	15% (w/v)	1:1
Sample 3(TrX1)	15% (w/v)	22.5% (w/v)	1:1.5
Sample 4(TrX1)	15% (w/v)	30% (w/v)	1:2

2.4 Apparatus

Some useful theoretical details regarding equipment could be found in this section.

2.4.1 Viscosity study: operational parameters and calculations

Viscosity measurement was performed on a Lamy Rheology Viscometer RM100 Plus with spindle MS-DIN 33 (concentric cylinder system) at a constant temperature of 20°C and a process time of 30 s. Five measurements were taken for each solution.

Since the polymer solution is driven through the electrospinning needle by the applied force due to the pump, the species in the solution may move faster near the axis of the needle and slower near the wall of the needle; which cause the generation of the shear stress [34]. The shear around the needle may cause newly formed molecular orientations, in other words, new hydrogen bonding patterns between polymer chains; which can change the rheological behavior of the solution [35]. Thus, non-Newtonian behavior of the polymer solutions led us to investigate the shear-dependent viscosity in this study [34,36]. The corresponding shear rates at the wall of the needle for each measurement was calculated from the flow rate through following equation [34,36]:

$$\dot{\gamma} = \frac{4Q}{\pi r^3}$$

where $\dot{\gamma}$ is the shear rate, Q is the flow rate (mL/min), and r is the radius of the needle (0.41 mm in this work). The viscosity measurements were made after the submission of the calculated shear rate values to the viscometer settings. All feed rates performed on electrospinning processes, corresponding shear rates calculated from the equation above and required rotating speed of the motor were given at Table 2.6.

Table 2.6 : The shear rate values calculated from the operational flow rates for viscosity measurement.

Flow Rate (uL/min)	Shear Rate (s^{-1})	Rotational Speed (rpm)
60	1.10	0.85
100	1.84	1.43
200	3.69	2.86
300	5.54	4.29
400	7.39	5.72
500	9.23	7.15

2.4.2 Studies of pH, conductivity and surface tension

The determination of each solutions' pH and conductivity was separately determined by Mettler Toledo SevenDirect SD23. The surface tension of all polymer solutions was investigated using the surface tension meter (GBX Instrumentation Scientific 3S). Five measurements were taken for each solution.

2.4.3 Electrospinning process and operational parameters

The nanofibers were fabricated by using the electrospinning machine Fluidnatek® LE-50. During the electrospinning process, different electrospinning parameters were used for each polymer solution. The solutions described in section 2.3 were supplied through a plastic syringe attached to a needle with an inner diameter of 0.41 mm.

Figure 2.6 : Image of the electrospinning machine.

A number of optimized electrospinning parameters; which were flow rate, needle to collector distance and applied voltage, are listed in Table 2.7 for each sample. The distance between tip and collector plate ranged between 10 to 22 cm and the applied voltage ranged from 16 to 25 kV. DOE - Design of Experiment 13 was used to determine the parameters for Sample 1, 2, 3 and 4. The electrospun fibers were calcined at 600 °C for 2 h by using a furnace (Nabertherm 30-3000 °C with P 330) with a heating rate of 0.5 °C/min.

Table 2.7 : The optimized electrospinning process parameters for each sample solution.

Sample Name	Needle to collecter distance (cm)	Flow Rate (uL/min)	Voltage (kV)
Sample 1	16	300	20
Sample 2	10	400	18
Sample 3	14.25	500	18
Sample 4	12.5	300	20
Sample 2(Ac)	15	100	18
Sample 2(Eth10)	10	300	16
Sample 2(Eth20)	10	500	25
Sample 2(TrX1)	22	200	20

2.4.4 Scanning electron microscopy (SEM) analysis and thermogravimetric analysis (TGA)

Electrospun nanofiber morphology was characterized by using Phenom ProX desktop scanning electron microscope (SEM). The diameter of electrospun nanofibers was measured using ImageJ and MATLAB R2022b.

Thermogravimetric analysis was carried out on PerkinElmer Thermogravimetric Analyzer TGA 4000. Nanofibers were heated from room temperature to 900 °C with an increase of 2 °C/min under N_2 atmosphere, the pressure was 2 bar.

3. RESULTS & DISCUSSION

3.1 Study of the PVA Solution Viscosity for Good Electrospinnability

There are several parameters that need to be in balance with each other for successful electrospinning process. Some of them can be adjusted during the electrospinning, for instance processing parameters such as voltage, tip to collector distance and flow rate; while others, such as concentration that belongs to the solution parameters, can be determined by investigating various concentrations. In order to start with the best concentration, several candidate polymer concentrations ranging from 7% to 20% (w/v) were prepared. Since the best solution among the candidates should be viscous enough for electrospinning operation, the viscosity of all samples was measured [37]. Table 3.1 displays the viscosity results at 20 °C. Figure 3.1 is the graph that was plotted from the data of Table 3.1, in order to show the effect of concentration on viscosity.

Table 3.1 : The Viscosity results of varying concentration of PVA solution.

	Concentration of PVA Solutions (w/v)			
Viscosity results (Pa.s) for flow rate 500	**7%**	**8%**	**9%**	**10%**
	0.016 ± 0.0009	0.022 ± 0,011	0.049 ± 0.0082	0.138 ± 0.0091
	11%	**12%**	**13%**	**14%**
	0.193 ± 0.0167	0.315 ± 0.012	0.472 ± 0,005	0.766 ± 0.0122
	15%	**16%**	**17%**	**18%**
	1.046 ± 0.0157	1.513 ± 0.0083	1.145 ± 0.0079	1.714 ± 0.0074
	19%	**20%**		
	2.344 ± 0.0111	2.316 ± 0.0266		

The concentration of the polymer solution has a direct effect on viscosity and surface tension [38]. These two parameters do not have a directly proportional relationship with each other; however, they are individually in balance with each other in the case of optimized electrospinning process, since the existing forces between solutes and solvent system determines the final level of the viscosity and surface tension.

At low concentration values of the polymer, the interaction between solvent molecules will be dominant with respect to those between solute ones because of the low entanglement degree of the polymeric chains. In this case, the surface tension will be

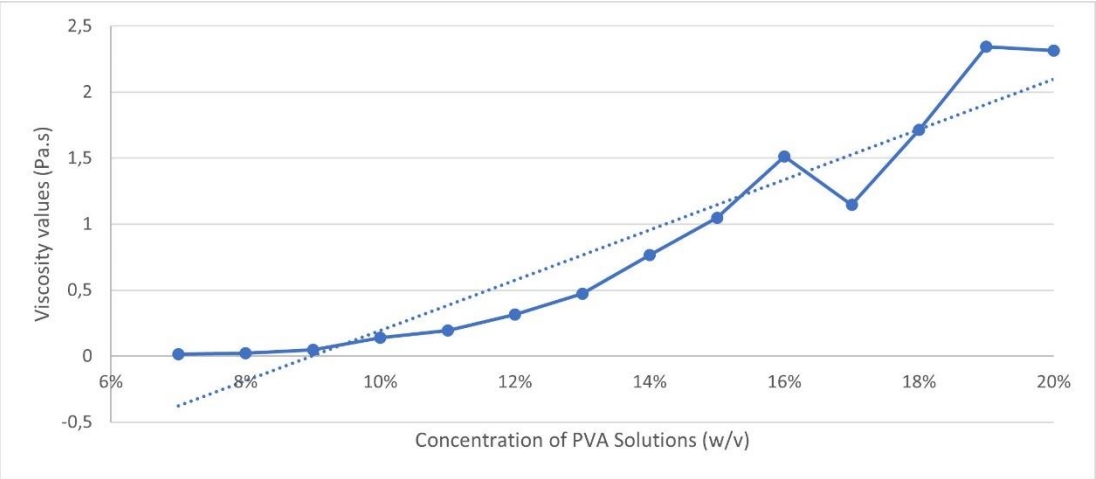

Figure 3.1 : The graph of PVA solution's viscosity results with respect to varying concentrations.

more crucial parameter than viscosity; and therefore, the adjustments to the surface tension will be the key point to a good electrosinnability because high values of surface tension may be the obstacle to spin with a low viscosity [31,32,33,38]. The initial data of the Figure 3.1 may be the example of aforementioned explanation; the spinnability of the solution was poor when the concentration varies between 7% and 10%.

As the increasing values of the concentration, especially after 10%, the change in viscosity also was increased at every point; except the concentration value of 17%. Probably, this was a measurement error or device-based error; therefore, that point can be excluded from the evaluation.

In the region where the viscosity was increased, the rate of the increase was more observable in some areas. This change can be understood by following the slope of the graph shown in Figure 3.1. As far as the slope of the concentration values of 11% to 13%, 13% to 15% and the 15% to 16% were considered individually, each of them had different slopes. In order to follow the change of slopes better, the highlighted version of the Figure 3.1 was displayed in Figure 3.2. The change of the slope between 11% to 13% and 13% to 15% was more dramatic; however, there was also partially increase between 13% to 15% and 15% to 16%. The change between these two regions could be considered as a transitional change of the concentration from moderate levels to sufficiently high levels. The entanglements existed at moderate levels; however, the electrospun nanofibers could have defects, in other words, it could be a mixture of beads and fibers since the surface tension had not been sufficiently overcome by the viscoelastic forces. Yet, the electrospun nanofibers with minimum defect could be

obtained at sufficiently high level of the concentration value; in the present case concentration of 15%, which refers to the desired level of the entanglement between the polymer chains [32,28].

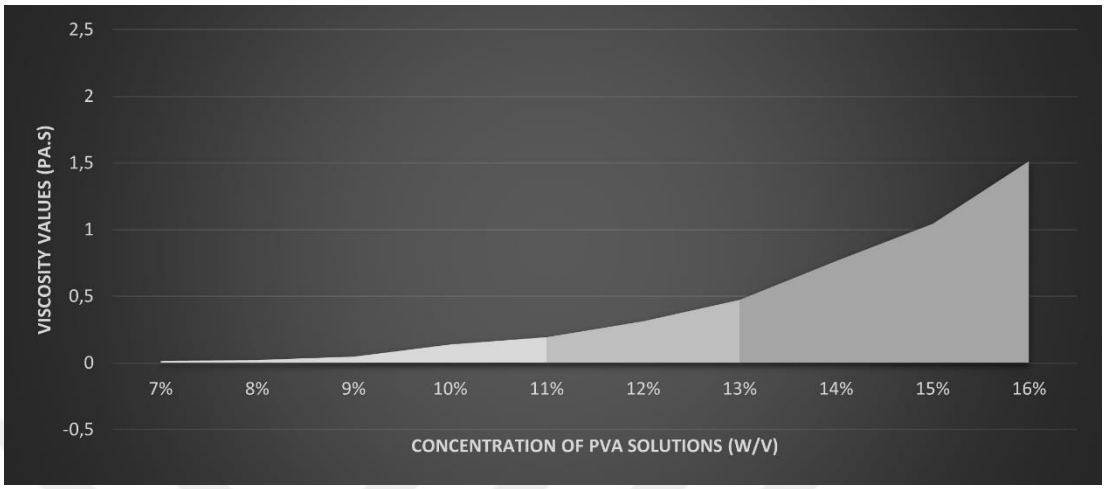

Figure 3.2 : Highlighted version of the previous graph.

There was also an increase in viscosity at the concentration region of 18% to 20%, but the slope of this region was almost identical to previous one. That is why, 15% (w/v) concentration for PVA was determined as the lower electrospinnable concentration and its solution was labeled as “Sample 0”.

3.2 The Study of the Polymer/Inorganic Precursor Species for Formation of Target Material, Zinc Oxide (ZnO) Nanofibers

In this part, the results of physicochemical and morphological analyzes of the PVA-zinc acetate dihydrate solution were given and these results were examined, compared and interpreted in order to get meaningful assumptions. Additionally, the thermal behavior of the precursor samples was also analyzed and evaluated through thermogravimetric analysis.

3.2.1 The physicochemical evaluation of the PVA-zinc acetate dihydrate solutions

In this set of experimental work; pH, conductivity, surface tension and viscosity of the samples having varied PVA – zinc acetate dihydrate mass ratios of 1:0.5, 1:1, 1:1.5 and 1:2 were investigated.

3.2.1.1 pH study: the formation and solubility of zinc hydroxide ($Zn(OH)_2$) in electrospinning solutions

Table 3.2 shows the pH values at each stage during the solution preparation. The decrease in pH after addition of zinc acetate dihydrate was common point for all prepared solutions. However, this decrease varied according to the amount of zinc acetate dihydrate added.

Table 3.2 : The pH measurements of PVA-zinc acetate dihydrate solutions: the pH of distilled water, the pH of solution after addition of Zinc acetate dihydrate (not containing PVA) and the pH of electrospinning solution.

Labels	PVA Conc. (w/v)	$Zn(OAc)_2{\cdot}H_2O$ Conc. (w/v)	pH of distilled water	pH after addition of $Zn(OAc)_2{\cdot}H_2O$	pH of electrospinning solution
Sample 1	15%	7.5%	7.56 ± 0.005	6.21 ± 0.013	6.08 ± 0.009
Sample 2	15%	15%	7.56 ± 0.005	5.93 ± 0.009	5.92 ± 0.009
Sample 3	15%	22.5%	7.56 ± 0.005	5.70 ± 0.004	5.72 ± 0.004
Sample 4	15%	30%	7.56 ± 0.005	5.57 ± 0.007	5.51 ± 0.007

The decrease in pH and the variability of this decrease could be explained by the reaction (6);

$$Zn^{2+} + 2OH^- \longleftrightarrow Zn(OH)_2 \qquad \text{reaction (6)}$$

The zinc ions coming from the dissolution of the zinc acetate dihydrate consumed the hydroxide ions (OH^-) that existed in aqueous medium in order to form zinc hydroxide as a solubility product [15,19]. The consumption of those hydroxide ions led to pH decrease. As the amount of Zn^{2+} ions coming from the salt increased, the pH decreased further. That is why; the pH values of Sample 1, Sample 2, Sample 3 and Sample 4 reached 6.21, 5.93, 5.70 and 5.57, respectively.

Indeed, the solubility of the $Zn(OH)_2$ in water depends on some parameters such as pH and temperature; it cannot dissolve in all conditions [39]. Reichle et al. found that zinc hydroxide has good solubility in two different pH regions at 25 °C: when the pH is around 7 and when the pH is higher than 12.5. Since the pH of Sample 1, Sample 2, Sample 3 and Sample 4 were close to the neutral region after the addition of zinc acetate dihydrate, any problems regarding the solubility of the zinc hydroxide was not observed. Thus, pure solutions were obtained. It should be mentioned that, reaction (6) was not an irreversible chemical reaction; that is why, all zinc ions coming from the inorganic salt dissolution were not participate to form the solubility product of

$Zn(OH)_2$. The free ions, Zn^{2+} and acetate (CH_3COO^-), could be present in the solutions along with $Zn(OH)_2$.

As far as the final pH values of 6.08, 5.92, 5.72 and 5.51 were concerned, a negligible difference was observed in the pH of the electrospinning solutions that were obtained as a result of the 2 h reaction of Sample 1, Sample 2, Sample 3 and Sample 4, respectively.

3.2.1.2 Conductivity study of the PVA-zinc acetate dihydrate solutions at each stage

Table 3.3 shows the conductivity values at each stage during the solution preparation. The conductivity of the solutions was increased almost directly proportional to the amount of dissolved salt of zinc acetate dihydrate. Only the conductivity of the Sample 3 was slightly higher than Sample 4. This might be a device-related error, the accuracy of the measurement might be affected adversely at high values of conductivity; or due to the result of the interaction of the dissolved ions with the polymer chains. Those interactions will be discussed in following sections.

Table 3.3 : The conductivity measurements of PVA-Zinc acetate dihydrate solutions at each stage: the conductivity of distilled water, the conductivity of solution after addition of Zinc acetate dihydrate (no PVA) and the conductivity of electrospinning solution.

Labels	PVA Conc. (w/v)	$Zn(OAc)_2 \cdot H_2O$ Conc. (w/v)	Conductivity of distilled water (µS/cm)	Conductivity after addition of $Zn(OAc)_2 \cdot H_2O$ (µS/cm)	Conductivity of electrospinning solution (µS/cm)
Sample 1	15%	7.5%	28.22 ± 0.43	15996.8 ± 352.91	7765.66 ± 46.59
Sample 2	15%	15%	28.22 ± 0.43	18811.02 ± 307.89	9788.88 ± 47.87
Sample 3	15%	22.5%	28.22 ± 0.43	19354.40 ± 316.13	10263.72 ± 40.17
Sample 4	15%	30%	28.22 ± 0.43	18950.18 ± 37.85	10174.40 ± 42.47

However, it is known that the conductivity of the solution has important effect on the surface charge on the jet. The jet carries more charges in a case where the electrical conductivity of the solution has higher values; that is why, the stretching of the electrospun jet and the bending instability will be changed [40]. Since the electrospinning set-up did not have any monitoring systems, the effects were followed by observing more stable taylor cone and jet formation at the tip of the needle with naked eye.

3.2.1.3 Viscosity study of the PVA-zinc acetate dihydrate solutions

Table 3.4 shows how viscosity changed at varying $Zn(OAc)_2 \cdot H_2O$ concentration in different feed rates. Except the viscosity results of the samples for the flow rate values for 60 and 100 uL/min, it could be said that the viscosity increased as the $Zn(OAc)_2 \cdot H_2O$ concentration increased. The instrumental error could be the reason for those measurements, since the viscosity values of all remaining measurements were increased in same behavior; they all increased with increasing $Zn(OAc)_2 \cdot H_2O$ concentration.

Table 3.4 : The viscosity chart for Sample 0, Sample 1, Sample 2, Sample 3 and Sample 4 in varying feed rates between 60 to 500.

Labels	PVA Conc. (w/v)	$Zn(OAc)_2$ Conc. (w/v)	Viscosity Results (Pa.s) for Flow Rate (F.R.)…		
			F.R. 60 uL/min	F.R. 100 uL/min	F.R. 200 uL/min
Sample 0	15%	0%	1.91 ± 0.053	1.56 ± 0.053	1.25 ± 0.012
Sample 1	15%	7.5%	1.69 ± 0.071	1.56 ± 0.079	1.35 ± 0.027
Sample 2	15%	15%	2.08 ± 0.073	1.92 ± 0.033	1.71 ± 0.021
Sample 3	15%	22.5%	2.50 ± 0.098	2.33 ± 0.089	2.06 ± 0.014
Sample 4	15%	30%	4.01 ± 0.078	4.01 ± 0.058	3.87 ± 0.079
			F.R. 300 uL/min	F.R. 400 uL/min	F.R. 500 uL/min
Sample 0	15%	0%	1.16 ± 0.013	1.12 ± 0.005	1.11 ± 0.014
Sample 1	15%	7.5%	1.28 ± 0.015	1.25 ± 0.003	1.25 ± 0.003
Sample 2	15%	15%	1.63 ± 0.020	1.60 ± 0.011	1.59 ± 0.006
Sample 3	15%	22.5%	1.99 ± 0.015	1.97 ± 0.014	1.99 ± 0.016
Sample 4	15%	30%	3.94 ± 0.099	3.93 ± 0.058	3.91 ± 0.072

The reason why this instrumental error was only seen at the measurements for flow rate 60 and 100 uL/min might be the low rotational motor speed of the viscometer. The instrument might also not be able to properly sense the response of the solution, as it rotates slowly enough to provide shear stress corresponding to the flow rates of 60 and 100 uL/min. At increasing values of shear stress and accordingly flow rates, the device might receive a sufficient response to the effect it applied; and therefore, the measured viscosity values became consistent to each other.

As it is known from the literature, the viscosity of the polymer solutions is directly related with the amount of polymer chains entanglement; and therefore, the molecular weight of the polymer and the concentration of the polymer solution [41]. Since all polymer solutions in this section of study were prepared at the same concentration by using the same PVA, the reason for the change in viscosity could not be

aforementioned parameters. The only reason was the addition of the zinc precursor salt, $Zn(OAc)_2 \cdot 2H_2O$, in different amounts. The dissolved ions of the salt, Zn^{2+} and CH_3COO^-, had different fates in aqueous solution. The effect of these ions on the surface tension will be discussed in the next section. In this section, only the effect on viscosity will be discussed.

Thanks to the pendant hydroxyl groups of PVA, the dominant physical interaction in the aqueous solution of the PVA was the hydrogen bonding. These hydrogen bonds could occur between chains as well as with water molecules [42]. The frequency of these two interactions might predominantly depend on the concentration of the solution and chain lengths, but also depended on some agents added to the solution up to some extent. Especially, the intra- and inter- chain bondings between polymer chains could be influenced when the metal ion, Zn^{2+}, was coordinated between the acceptor side of hydrogen bonds [43,44]. Such coordination might affect the existing hydrogen bondings and also lead to the formation of new hydrogen bonds both in intra- and inter-molecular levels. Since all kind of new formations would increase the interactions between chains in both cases, it is possible to say that a new physical cross-linking network could be formed in some parts of polymeric interactions [45]. Such physical cross-links could also be accepted as a kind of physical entanglement since they do not have covalent bond characteristics. Since the entanglements between polymer chains at a constant polymer concentration might increase due to the zinc ions existing in aqueous medium, the viscosity of the solution also might increase depending on the increasing zinc ion concentration deriving from the zinc acetate dihydrate dissolution.

3.2.1.4 Surface tension study of the PVA-zinc acetate dihydrate solutions

Surface tension is a property that defines about the liquid surface and one of the parameters that must be overcome in the electrospinning process. In order to evaluate this parameter, the focus should be gathered on all possible interactions of liquid molecules; both the interactions between liquid molecules and the interactions with solute species [31,32]. That is the reason why, not only the electrospinning solutions with varied concentration of $Zn(OAc)_2 \cdot H_2O$ were examined, but also the surface tension of distilled water and the polymer solution of Sample 0 were examined for

comparable evaluation in order to investigate the effect of each element in the aqueous medium.

Before starting the surface tension measurements of the polymer solutions, the surface tension of the distilled water was measured; it was found 73.75 mN/m. Table 3.5 showed that, the surface tension decreases in all polymer solutions regardless of $Zn(OAc)_2 \cdot H_2O$ addition. The reason might be the interactions of some of the polymer chains on the solution surface.

Table 3.5 : The surface tension results for all electrospinning solutions of Sample 0, Sample 1, Sample 2, Sample 3 and Sample 4.

Labels	PVA Conc. (w/v)	$Zn(OAc)_2 \cdot H_2O$ Conc. (w/v)	Surface Tension (mN/m)
Sample 0	15%	0%	45.42 ± 0.230
Sample 1	15%	7.5%	36.31 ± 0.560
Sample 2	15%	15%	38.61 ± 0.881
Sample 3	15%	22.5%	46.23 ± 0.730
Sample 4	15%	30%	51.42 ± 1.562

Before the polymer was added, the water molecules made hydrogen bonds between themselves. Having been added the PVA; besides the existing hydrogen bonds formed among water molecules, the pendant hydroxyl groups also made hydrogen bonds with water molecules and this led to new orientations between water molecules at the surface [42]. Since the interactions between water molecules at the surface were interrupted by the PVA chains, a decrease in surface tension was observed.

Another information seen in Table 3.5 was the change in surface tension values depending on the precursor zinc salt concentration ($Zn(OAc)_2 \cdot H_2O$). It was observed that the surface tension decreased to 36.31 mN/m from 45.42 mN/m, when half equivalent of the salt, Sample 1**,** was added to the PVA solution. Afterwards, a continuous increase in surface tension values was observed depending on the amount of salt. The value of this increase was less compared to the PVA solution without salt, Sample 0, up to a certain point. In the case where the equivalent salt concentration was 1:1.5, Sample 3, the surface tension value (46.23 mN/m) became more or less equal with respect to the surface tension value of Sample 0. However, the surface tension value of Sample 4 (51.42 mN/m), which had double equivalent amount of salt with respect to the amount of PVA, was relatively higher. The existing interactions of all species in aqueous medium could explain how all these affected the surface tension.

The dissolved ions of the salt, Zn^{2+} and CH_3COO^-, had different effects on surface tension. Acetate ions could form hydrogen bonds with water since they were hydrogen bond acceptor. As in all parts of the solution, those newly formed hydrogen bondings would interrupt the highly structured and extensive network of hydrogen bonds of water, and these new bonds were expected weaker than previous ones since acetate ions were larger than water molecules [46,47,48]. It can be concluded that acetate ions could reduce the surface tension of the solution through its hydrogen bonding ability.

However, those interactions were specific between water and acetate ions. The interactions of the acetate with polymer chains, and more notably, the interactions of the PVA chains with zinc ions should also be taken into account, since acetate ions were not the only ions that derived from the dissolution of $Zn(OAc)_2 \cdot H_2O$. There were also zinc ions in the medium. It should be noted again that reaction (6) was not irreversible reaction and there were some zinc ions in the aqueous medium that were not consumed by the hydroxide ions in order to form $Zn(OH)_2$. As mentioned in the viscosity studies section, zinc ions could increase the interaction between polymer chains, in such a way as weak physical crosslinkers. The increase of zinc ions could prevent the migration of the polymer chains from the bulk to the surface up to a certain point thanks to aforementioned role in the medium. This migration could be dominantly seen in especially pure polymer solutions, in other words, the polymer solutions containing only water and polymer molecules due to following reason. Since water molecules have a strong affinity to associate with one another through hydrogen bonds, PVA molecules would stay at a higher free-energy state, which is the characteristic of the bulk of the solution according to mentioned conditions [42]. Thus, PVA chains would always migrate from the bulk to the surface; in other words, to a lower free-energy condition. The water molecules on the surface would no longer interact only with themselves, but also with the polymer chains migrated to the surface. Decrease in surface free energy was the result of accumulation in the surface of those molecules with weaker fields [42]. Zinc ions, which increase the physical interaction between the PVA chains, could retard this migration up to a certain point. That is why; the increasing zinc concentration, accordingly $Zn(OAc)_2 \cdot H_2O$ concentration, could also increase the surface tension of the polymer solution.

As far as the mentioned mechanisms for describing the effect of $Zn(OAc)_2 \cdot H_2O$ addition on the surface tension were concerned, the effects of other parameters such

as temperature and pH had also an effect on these mechanisms since they have influence on any kind of physical interactions between polymer chains and hydrogen bond formation between all kind of species in the medium [42,44,46]. Therefore, the surface tension of electrospinning solutions is a rather complex and complicated. However; if only the effect of dissolved salt is considered, the overall effect of adding zinc acetate dihydrate should be taken into account: the balance between the physical cross-linking effect of zinc ions and the surface tension reducing effect of acetate ions. The increase in the surface tension of electrospinning solutions containing zinc acetate dihydrate defined that the effect of zinc ions on this balance was more; the effect of acetate ions on reducing surface tension might be overwhelmed by the effect of zinc ions, resulting in an increase in surface tension.

3.2.2 The thermogravimetric analysis of samples and the formation of ZnO nanofibers

In order to determine the calcination temperature of the electrospun membrane, thermogravimetric analysis (TGA) of Sample 0 was done, it was heated up to 900 °C with an increase of 2 °C/min under N_2 atmosphere. At first glance, it was observed that there were two peaks in the TGA graph; seen in Figure 3.3. If the 5% weight loss was accepted as the beginning of the decomposition, the onset of early decomposition of Sample 0 was around 250 °C; which is also the onset of the first peak [49]. A sharp decrease in weight continued up to around 326.5 °C; at which temperature almost 75% of the analyzed sample was decomposed. The reason of the faster decomposition was probably due to the degradation of the amorphous regions, as they are less ordered and less densely packed regions. However, decomposition of the sample still continued after that temperature, but in slow manner. Although a shoulder on the peak around 400 °C was observed, it could be considered as a part of the phenomena that occurred until the end of total decomposition, not a separate phenomenon. In addition, it was seen that the 90% of all sample was decomposed at around 482.4 °C and 95% of all sample was decomposed at 600 °C. The reason for both the shoulder revealed around 400 °C and the slower degradation, in other words the existence of second decomposition peak, might be the heating rate of the method. Since the gradient was low, heating rate was also slow and this might lead to phase transitions and/or rearrangement all of molecular interactions. Thanks to them, crystalline regions of the

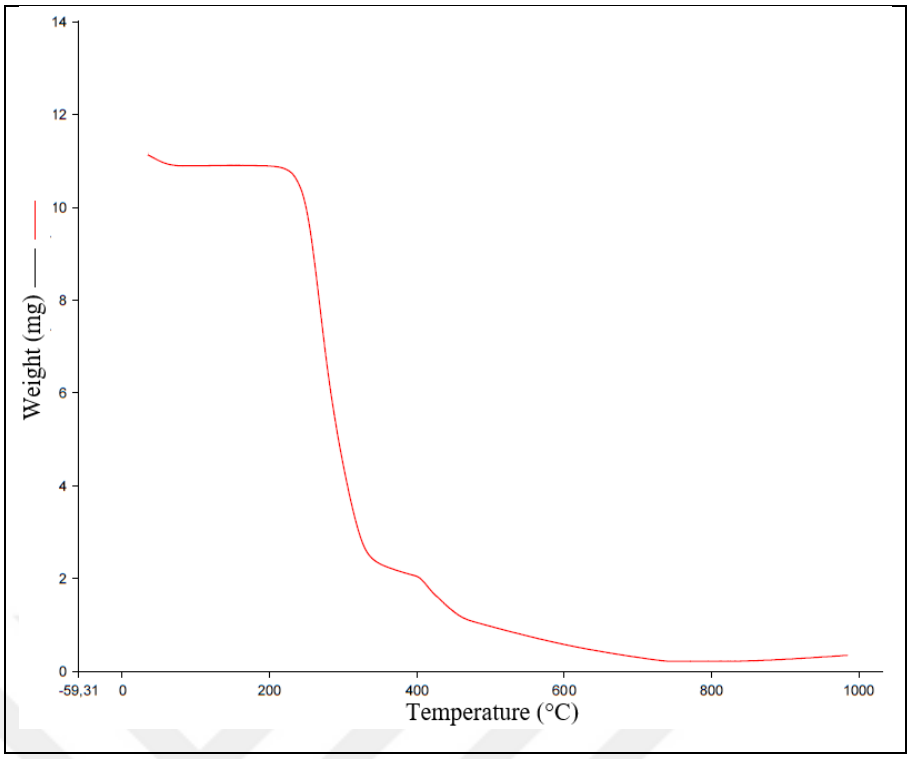

Figure 3.3 : The thermogravimetric analysis (TGA) graph of PVA-based sample.

polymer matrix rearranged and resulted to the formation of more ordered and more densely packed regions that led to delay for decomposition of PVA. It was observed that the whole sample completely decomposed at around 735.3 °C.

Having added zinc acetate dihydrate to the PVA solution, three peaks were observed in the TGA graph instead of two peaks. However, this was not the only difference that was observed; many shifts in temperature values regarding decomposition, both onset and end, and change in decomposition rate also observed in this case.

At the point at which 5% of the total weight was lost, the temperature value was around 116 °C. However, this weight loss was probably referred to water loss; since it was too low compared to the data that was driven from Sample 0. If the data obtained from the graph shown in Figure 3.3 had been considered as a reference, the peak that started at around 213.4 °C should belonged to the decomposition of the amorphous regions; because the characteristic, which is a sharp decrease in weight, was identical to the peak that derived from previous finding. Figure 3.4 indicates that 85 % of the initial mass was present at the onset of the decomposition of amorphous region, 213.4 °C; however, at the end of this peak, around 234.8°C, only 61,8 % of the total mass

remained in the environment. Now, a comparison can be made in order to understand how zinc acetate dihydrate addition affected the rate of degradation.

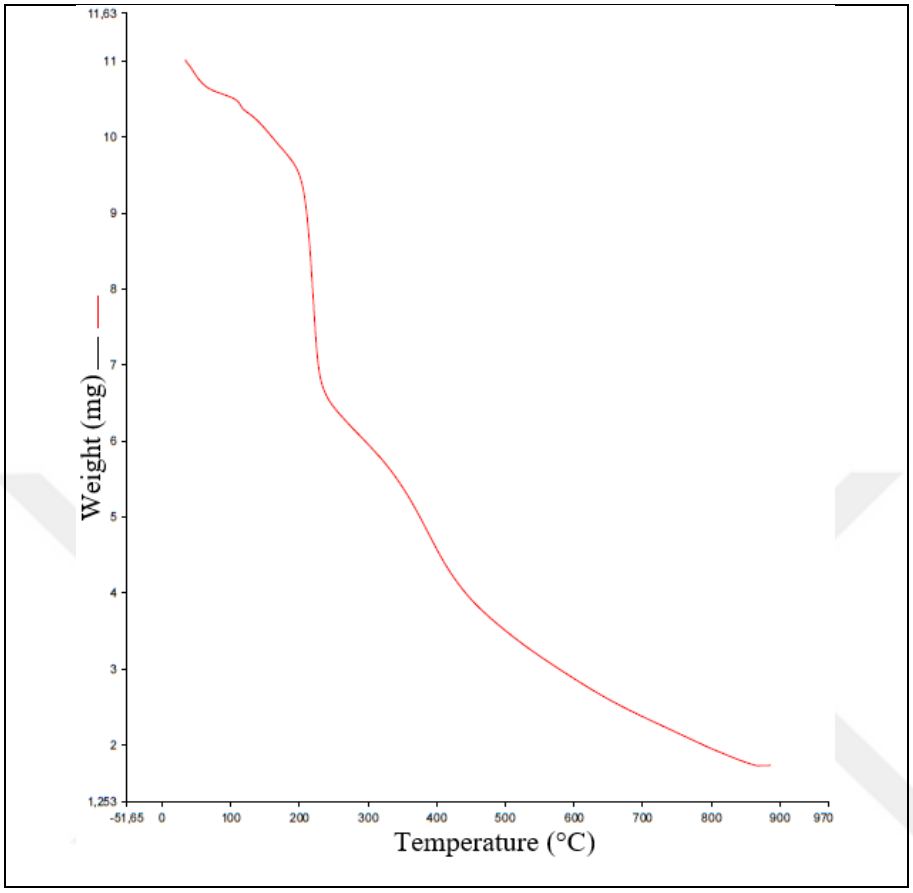

Figure 3.4 : The thermogravimetric analysis (TGA) graph of PVA- $Zn(OAc)_2 \cdot 2H_2O$ sample.

The temperature at which 61.8 % of the Sample 0 was remained corresponds to around 279.4 °C; which was higher than 234.8°C. If the same amount of decomposition occurred at a lower temperature when zinc acetate dihydrate was added, it could be concluded that zinc acetate dihydrate addition had an accelerating effect on decomposition rate. This might be due to the rearrangement of polymer chains by the influence of zinc ions and zinc species that were derived. The randomly oriented and packed chains in amorphous region probably became more random because of the interference of zinc species. However; the effect of this interference was also seen in further stages. Since the temperature gradient is low, chains probably could find the opportunity for rearranging with each other as well as zinc species in the medium; which led to formation of crystalline regions.

In the case of samples that had precursor zinc salt content, it was very difficult to follow the degradation of the polymer by weight loss; because even at 900 °C, towards

the end of the analysis, about 16% of the total mass remained in the environment. This residual mass probably belonged to the inorganic species, since the hydrocarbons cannot exist until that temperature. The aforementioned inorganic species was ZnO and it is known that ZnO could be formed through intermediate product of $Zn(OH)_2$ by potential reactions. One of these might be the reactions of (7), (8) and (9); reactions occurred in aqueous medium. Although those reactions required basic medium and a certain minimum temperature, 80°C, some ZnO might be formed through them even with slight possibility as an aqueous medium product [17]. However, the main formation reaction of ZnO was thought via a thermal decomposition reaction as described below [19]:

$$Zn(OH)_2 \xrightarrow{\Delta} ZnO + H_2O \qquad \text{reaction(10)}$$

As it can be seen in the above reaction, ZnO is formed by the elimination of water from $Zn(OH)_2$, in other words, the formation of ZnO occurred through a weight loss. According to the literature, the formation of this reaction is above 460 °C [50]. Moreover, as the temperature of thermal process increases, the size of the newly formed ZnO crystals also increases; even at 700 °C [51]. Therefore, evaluating TGA graph of $Zn(OH)_2$ containing samples were complicated because the late degradation of the PVA and the formation of ZnO occurred simultaneously. The peaks arising from the mentioned formations could be observed in Figure 3.4, especially after 448°C, at which remaining mass was around 35,5%. According to the data from the previous graph shown in Figure 3.3, this temperature range was the region where the end of the decay was observed, as 90% of the initial sample was lost at 482.4 °C. Since the zinc species containing samples degraded faster and therefore there was a shift in temperature values, 448°C and above could be considered as a range in which the final stage of the degradation of the hydrocarbon content was experienced. Certainly, the decomposition of $Zn(OH)_2$ accompanied with it. Within the range of the last peak in Figure 3.4, the temperature at which the 50% weight loss detected was 610 °C; which could be accepted as calcination temperature of the current sample.

3.2.3 The morphological study: SEM analysis of the samples at pre- and post-calcination processes

SEM analysis was performed on both freshly formed samples after electrospinning process, which refers to pre-calcination step, and the samples obtained after the

calcination process. The aim here was to conduct morphological investigation of the final structures, as well as fiber diameter analysis and elemental analysis.

The SEM images of the Sample 1 obtained before and after the calcination process could be seen in Figure 3.5.

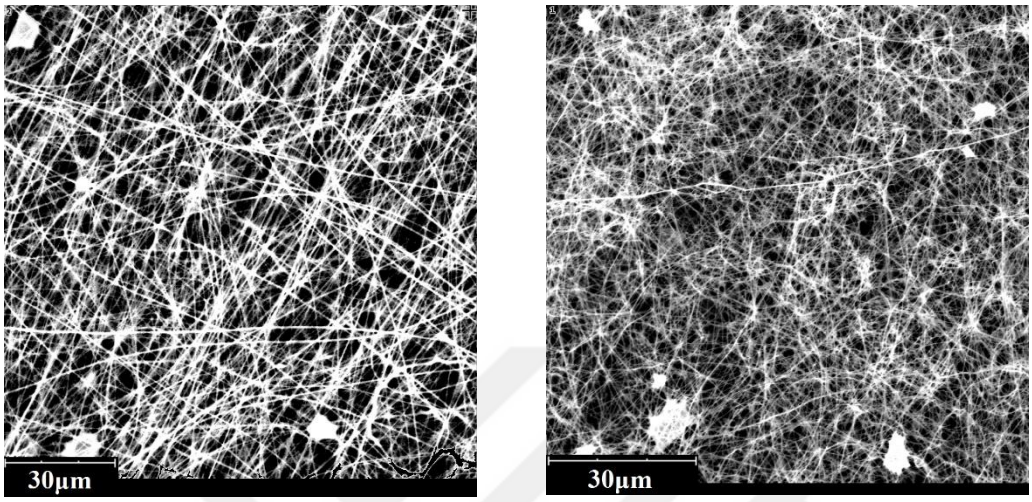

(a) (b)

Figure 3.5 : The SEM images of Sample 1; before (a) and after (b) calcination at scale 30µm.

Sample 2 was also analyzed to observe the morphological changes that might be occurred when mass ratio of zinc salt precursor was doubled. The SEM images of the Sample 2 obtained before and after the calcination process could be seen in Figure 3.6.

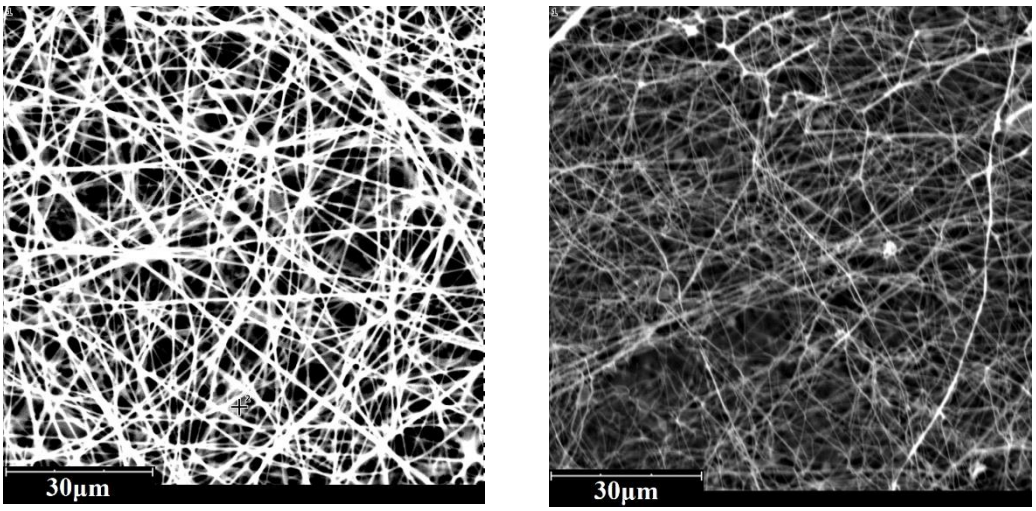

(a) (b)

Figure 3.6 : The SEM images of Sample 2; before (a) and after (b) calcination at scale 30µm.

The morphological effect of the mass ratio of 1:1.5 (PVA: $Zn(OAc)_2 \cdot H_2O$) on electrospun structure was also analyzed. The SEM images of the Sample 3 obtained before and after the calcination process could be seen in Figure 3.7.

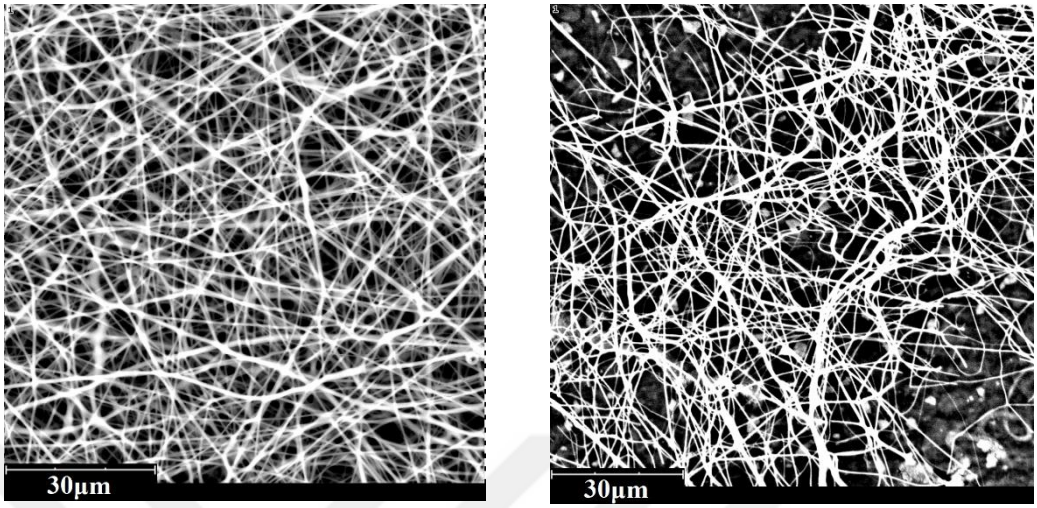

(a) (b)

Figure 3.7 : The SEM images of Sample 3; before (a) and after (b) calcination at scale 30µm.

Finally, morphological investigation of the mass ratio of 1:2 (PVA: $Zn(OAc)_2 \cdot H_2O$) was done to make comparison between all samples. The SEM images of the Sample 4 obtained before and after the calcination process could be seen in Figure 3.8.

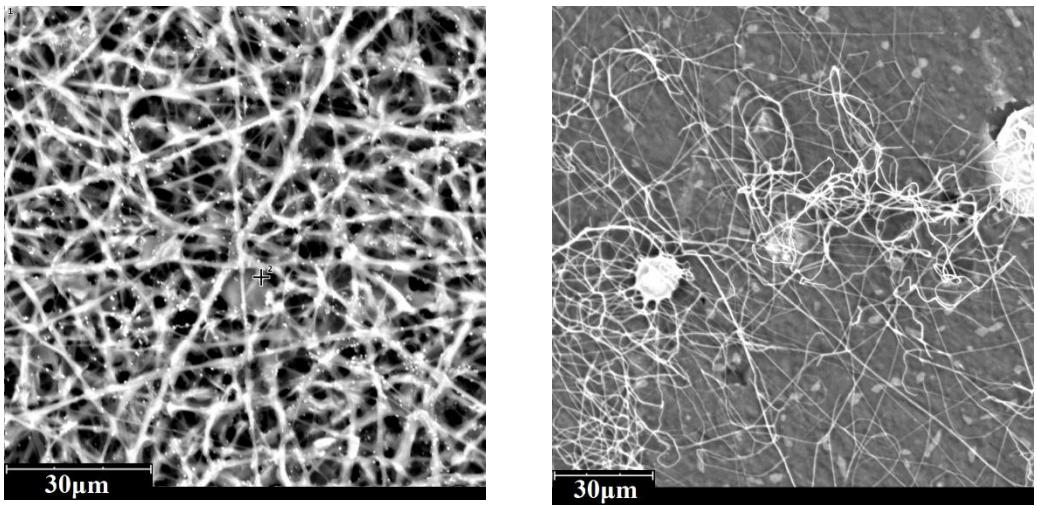

(a) (b)

Figure 3.8 : The SEM images of Sample 4; before (a) and after (b) calcination at scale 30µm.

3.2.4 The evaluation of the SEM results and decision of the best sample for gas sensing test

All diameters of Sample 1, Sample 2, Sample 3 and Sample 4 before and after calcination processes were summarized in Table 3.6 according to the data stated in Appendix A. The thickness of all samples varied depending on the amount of precursor zinc salt added. The fiber diameter of Sample 1, 2, 3 and 4 were proportionally increased with the increasing concentration of zinc acetate dihydrate for both pre- and post- calcination processes. Since the membrane that obtained after calcination would be used in gas sensing test, evaluation of the data of post-calcination process was more important.

Table 3.6 : The diameter of all samples both pre- and post- calcination phases.

Sample Name	Diameter before Calcination (μm)	Diameter after calcination (μm)
Sample 1	0.851 ± 0.105	0.398 ± 0.080
Sample 2	0.870 ± 0.173	0.632 ± 0.090
Sample 3	0.974 ± 0.162	0.643 ± 0.098
Sample 4	1.116 ± 0.221	0.721 ± 0.137

More sensitive and precise gas measurement tests could be done by synthesizing more ZnO-containing membrane; however, the fineness of the fiber was also another important parameter for measurement performance. The higher sensitivity is also obtained as surface area to volume ratio increases, and this can be possible as the fiber diameter lowers [16,20,21,22]. In light of mentioned points, Sample 2 and Sample 3 could be ideal candidates for being testing element. The average fiber diameter of former was 0.632 μm ± 0.090, while the latter was 0.643 μm ± 0.098. Among these two options, which were very close to each other, it would be appropriate to choose the Sample 2 since it was obtained by consuming less chemicals.

However, there was a second reason that led to this choice. During the electrospinning process, the continuity and stability at the region of taylor cone and jet were not found satisfactory enough. The more amount of zinc acetate dihydrate added, the more mentioned instability was observed. Therefore, the Sample 2 having mass ratio of 1:1 offered better operational performance compared to the Sample 3 having mass ratio of 1:1.5.

Yet, the problem of the continuity and stability was a bit time consuming and adversely affected the manufacturing productivity. In the following sections, various attempts had been made in order to get a more optimized electrospinning process.

3.3 The Efforts for Better Electrospinning Process in order to Improve the Nanofiber Fabrication of PVA

Considering the formation mechanism and the fate of template substances ($Zn(OH)_2$ and PVA) throughout all stages before calcination; new solutions and solvent systems (such as acetic acid and ethanol solutions) and surfactant addition were applied to the selected regular electrospinning solution, Sample 2. Although no results were obtained due to the conflict between the possible formation mechanism of $Zn(OH)_2$ and PVA, the behavior of the Sample 2 in the basic medium was also examined.

3.3.1 Studies in acidic region

As far as the possible effects of acidic environment on solution in terms of both solute and solvent aspects were concerned, the pH of electrospinning solution Sample 2 was adjusted to 3,5; accordingly, Sample2(Ac) was prepared for investigation.

As a result of visual assessment, the solution was considered to be homogeneous since Sample2(Ac) was as transparent as Sample 2. It was expected that acid addition would create new hydrogen bonding probabilities both with water molecules and polymer chains and lead to new formations that might affect the solution property. Table 3.7 shows the results of the physicochemical studies of acidic region.

Table 3.7 : The pH and conductivity results of Sample2(Ac) for each preparation step.

Stages	pH	Conductivity (µS/cm)
1- Before $Zn(OAc)_2 \cdot H_2O$ addition	1.96 ± 0.007	811.34 ± 1.67
2- After $Zn(OAc)_2 \cdot H_2O$ addition	3.49 ± 0.007	14011.74 ± 359.54
3- Electrospinning solution	3.55 ± 0.013	6253.36 ± 41.82

Having done some trials, it was seen that the pH of the solution reached to almost 3.5 after $Zn(OAc)_2 \cdot 2H_2O$ addition if 4M acetic acid solution was used instead of pure distilled water as a solvent. The initial pH of 4M acetic acid solution was around 1.96. The addition of zinc precursor salt led to pH rise, 3.49. This increase was probably due to the protonation of the acetate ions which were arisen from $Zn(OAc)_2 \cdot 2H_2O$. Some of the hydronium ions that were present in acidic medium probably were consumed

for protonation of dissolved acetate ions and this consumption led to pH increase. Thus, there were much more acetic acid molecules in the medium compared to acetate ions. The protonation of acetate ions, which used to interrupt both potential intra- and inter- hydrogen bonds between PVA molecules, might mean that these potential interactions were possible in acidic environment. Consequently, the acetic acid molecules formed by the protonation of acetate ions would increase the interaction between the PVA chains, and accordingly would increase the interaction with water molecules [52].

The acidic environment did not have only effect on acetate ions, especially in this study. As it is known, the concentration of hydronium ions in an acidic medium is much higher than the concentration of hydroxide ions; and this would directly affect the reaction (6) quantitatively. Since the amount of hydroxide ions was very limited compared to the regular solutions; regardless the abundance of the zinc ions in the medium, much less Zn^{2+} would be consumed for the formation of $Zn(OH)_2$. This would increase the amount of residual zinc ions in the environment. As discussed in the previous section 3.2.1.3, zinc ions had a kind of physical cross-linking effect that increased the interactions between chains, which were basically similar to increase of chain entanglements; and those increase led to also increase in viscosity. This increase also could be observed experimentally for each flow rate values when the viscosity measurement results of Sample 2 and Sample 2(Ac) were examined. The viscosity investigation results of Sample 2(Ac) were defined in Table 3.8. More specifically; the viscosity of Sample 2 increased from 1.92 Pa.s ± 0.033 to 2.819 Pa.s ± 0.038 in the case of flow rate 100 uL/min, which was the optimum flow rate parameter for electrospinning of Sample 2(Ac).

Table 3.8 : The viscosity chart for Sample2(Ac) in varying feed rates between 60 to 500.

	Viscosity Results (Pa.s) for Flow Rate (F.R.)…		
Sample 2(Ac)	**F.R. 60 uL/min**	**F.R. 100 uL/min**	**F.R. 200 uL/min**
	3.095 ± 0,088	2.819 ± 0.038	2.559 ± 0.043
	F.R. 300 uL/min	**F.R. 400 uL/min**	**F.R. 500 uL/min**
	2.407 ± 0,021	2.416 ± 0.006	2.462 ± 0.012

Even if Sample 2(Ac) was not found appropriate to proceed in order to be used in gas sensing tests, the morphological effect of the acidic environment on electrospun structure was also analyzed. Since the viscosity results in acidic medium were higher

with respect to the results of regular solution, which therefore caused unsatisfactory electrospinnalibity; no further progress was made with this path. Thus, the calcination process was not performed. The morphological study of the electrospun acidic product was examined in order to observe the changes before passing other alternative attempts. The SEM images of the Sample 2(Ac) obtained before the calcination process could be seen in Figure 3.9. The fiber diameter analysis belonged to the SEM image of electrospun membrane Sample 2(Ac) indicated that the average fiber diameter and the standard deviation was 0.8573 μm ± 0.2084.

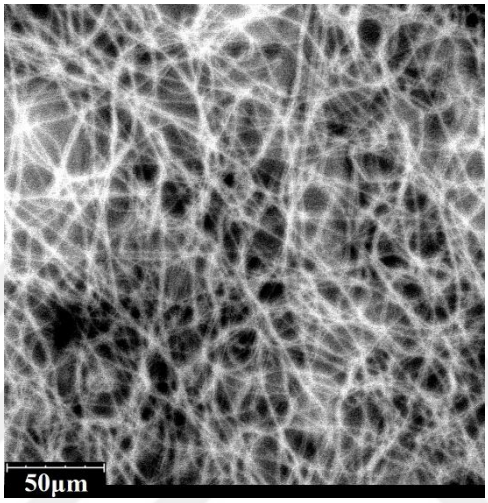

Figure 3.9 : The SEM image of Sample 2(Ac) before calcination at scale 50μm.

3.3.2 Studies in basic region

The second attempt for better electrospinnability was performed in the basic region. It was very difficult to determine the optimum parameters in basic conditions since the behavior of the PVA and aqueous product $Zn(OH)_2$ under basic conditions was totally different. The solubility of the $Zn(OH)_2$ depends on parameters such as pH and temperature; and as indicated in the Table 3.9, the solubility of zinc at 25 °C is poor between pH 8 – 12. The region in which pH is lower than 8, which is one of the two regions where $Zn(OH)_2$ has good solubility, already corresponded to our working range. For this reason, it was necessary to work in the range where the pH is higher than 12 in order to get some result in basic conditions. However, the viscosity problem of PVA solution was arisen; the polymer solution had lost its viscosity. Probably, hydroxyl groups of PVA were deprotonated by added base and newly formed deprotonated hydroxyl groups caused repulsion between chains, which directly

affected the sharp decrease in solution viscosity [53]. In conclusion, finding an optimum range was not possible since there is no optimum intersection between good enough solubility of $Zn(OH)_2$ and good enough viscosity of the polymer solution. Since an investigation could not be performed under basic conditions, SEM analyzes could not be performed either.

Table 3.9 : The solubility* chart of zinc hydroxide (adapted from Ref. [39]).

12.5 °C		25 °C		50 °C	
pH	S ($x10^5$)	pH	S ($x10^5$)	pH	S ($x10^5$)
13.8	327	13.19	178	12.5	261
13.71	216	12.97	67.3	12.24	88.7
13.51	91.8	12.77	28.3	11.99	33.7
13.34	45.1	12.52	11.2	11.76	14.8
13.18	25.2	12.29	5.74	11.55	8.03
12.85	6.12	11.05	0.54	11.25	2.92
12.21	1.68	10.84	0.46	10.99	2.14
11.51	0.50	10.14	0.31	10.75	1.38
11.50	0.31	9.43	0.38	10.25	0.92
11.10	0.24	9.18	0.54	10.02	0.84
9.83	0.23	8.97	0.61	9.55	0.76
9.49	0.23	8.91	0.92	9.08	0.87
9.27	0.31	8.72	0.84	8.77	0.99
9.14	0.38	8.67	1.22	8.52	1.15
8.99	0.46	8.41	1.30	8.27	1.45
8.55	1.33	7.90	4.74	8.04	1.84
7.96	13.2	7.63	17.2	7.82	2.43
7.70	48.3	7.44	32.1	7.54	4.97
7.32	265	7.31	49.7	7.26	10.7
7.22	415	7.00	204	7.05	19.6
7.06	844			6.75	53.4

*S represents the solubility expressed in mol of zinc per kg of water.

3.3.3 The effect of ethanol: studies on (90:10) and (80:20) water:ethanol binary solvent systems

In order to investigate the effect of the binary solvent system on electrospinning process, ethanol was also added as a solvent thanks to its perfect miscibility with water. It was not used as a single solvent since PVA and zinc acetate dihydrate were slightly soluble in ethanol [54].

Even at those concentration values where the ethanol ratio in the binary solvent system was higher than or close to the water ratio, some undissolved solutes were observed in the solutions. For this reason, two different variations of Sample 2 solutions; Sample 2(Eth10) with ethanol concentration of 10% (v/v) and Sample 2(Eth20) with ethanol concentration of 20% (v/v), were prepared to investigate the potential effects of hydrogen bondings that formed through both between solvent and solute molecules; and therefore, the possible effect on improving the nanofiber fabrication of electrospinning solution.

The visual assessment of the solution transparency stated that both Sample 2(Eth10) and Sample 2(Eth20) were homogenous. The results of the physicochemical investigations regarding pH and conductivity were stated below in Table 3.10 and Table 3.11 for samples Sample 2(Eth10) and Sample 2(Eth20), respectively.

Table 3.10 : The pH and conductivity results of Sample 2(Eth10) for each preparation step.

Stages	pH	Conductivity (µS/cm)
1- Before $Zn(OAc)_2 \cdot H_2O$ addition	6.306 ± 0.005	5.34 ± 0.055
2- After $Zn(OAc)_2 \cdot H_2O$ addition	5.884 ± 0.005	13000.38 ± 227.28
3- Electrospinning solution	5.864 ± 0.005	5986.68 ± 25.97

Table 3.11 : The pH and conductivity results of Sample 2(Eth20) for each preparation step.

Stages	pH	Conductivity (µS/cm)
1- Before $Zn(OAc)_2 \cdot H_2O$ addition	6.476 ± 0.0055	4.06 ± 0.055
2- After $Zn(OAc)_2 \cdot H_2O$ addition	5.85 ± 0.004	8336.46 ± 126.30
3- Electrospinning solution	5.83 ± 0.009	3724.34 ± 5.97

Although the pH of the virgin binary solvent system decreased to 6.3 – 6.6 range, the pH decrease resulting from the $Zn(OH)_2$ formation also was seen in both ethanol/water solutions, in the same way that seen in regular solutions. The pH values of Sample 2(Eth10) and Sample 2(Eth20) after $Zn(OAc)_2 \cdot 2H_2O$ addition were found 5.884 ± 0.005 and 5.85 ± 0.004 respectively; which were almost similar to the pH value of Sample 2 (5.926 ± 0.009) at the same stage. However, the similarity observed in in pH measurements was not observed in the conductivity measurements. Since the conductivity of organic solvents is low, a decrease in the conductivity of the ethanol/water solutions was observed depending on the concentration of ethanol [55]. As it was known from previous study, the conductivity of electrospinning solution

Sample 2 was 9788.88 μS/cm ± 47.87; however, it was measured 5986.68 μS/cm ± 25.97 for Sample 2(Eth10) and 3724.34 μS/cm ± 5.97 Sample 2(Eth20). Maybe, the reason why the electrospinning process of the latter was more unstable around the taylor cone and jet formation compared to the former might be the decrease in conductivity. That is the reason why, the solutions in which ethanol concentration was more than 20% (v/v) were not evaluated.

The results of the viscosity investigations of Sample 2(Eth10) and Sample 2(Eth20) were stated in Table 3.12 and Table 3.13. After the examination of the results, it was observed that the viscosity also changed depending on the amount of ethanol in the solution. The viscosity of the solution increased as the amount of ethanol in the solution increased. There might be two reasons for this increase. One of them might be the new formations of hydrogen bondings arisen because of the ethanol; in particular, new hydrogen bonds that increased the interaction between chains could cause an increase in viscosity. Another possibility could be the increase of free Zn^{2+} ions in the both solutions. Since the concentration of the distilled water in the binary solution systems were less than regular ones, the zinc ions released from the dissolution of the zinc acetate dihydrate would be react with less amount of hydroxide ions existed in the aqueous medium. Therefore, the amount of $Zn(OH)_2$, the product of reaction (6), would be less. Since less Zn^{2+} ions were consumed for this reaction, the amount of free Zn^{2+} ions in the environment would also be higher; and this might have an effect of increasing viscosity in a same manner described in section 3.2.1.3.

Table 3.12 : The viscosity chart for Sample 2(Eth10).

	Viscosity Results (Pa.s) for Flow Rate (F.R.)…		
Sample 2(Eth10)	**F.R. 60 uL/min**	**F.R. 100 uL/min**	**F.R. 200 uL/min**
	2.455 ± 0.0142	2.278 ± 0.060	1.948 ± 0.023
	F.R. 300 uL/min	**F.R. 400 uL/min**	**F.R. 500 uL/min**
	1.873 ± 0.006	1.826 ± 0.007	1.810 ± 0.007

Table 3.13 : The viscosity chart for Sample 2(Eth20).

	Viscosity Results (Pa.s) for Flow Rate (F.R.)…		
Sample 2(Eth20)	**F.R. 60 uL/min**	**F.R. 100 uL/min**	**F.R. 200 uL/min**
	2.878 ± 0.061	2.632 ± 0.070	2.264 ± 0.038
	F.R. 300 uL/min	**F.R. 400 uL/min**	**F.R. 500 uL/min**
	2.155 ± 0.020	2.081 ± 0.010	2.087 ± 0.022

The morphological effect of the binary solvent system on electrospun structures obtained from Sample 2(Eth10) and Sample 2(Eth20) were also analyzed. Before evaluating the results, it was necessary to declare that the electrospinning performance of the sample containing 10 % ethanol was slightly better than the sample containing 20% ethanol. The processibility of Sample 2(Eth20) was not as continuous as the Sample 2(Eth10) and required more intervention throughout the process. Also, SEM analysis result of the Sample 2(Eth20) was not clear enough to be evaluated. That is why, the candidate sample to be created for gas test produced from Sample 2(Eth20) was not studied further.

Figure 3.10 (a) and Figure A.6 show the SEM image and fiber analysis result of Sample 2(Eth10) before the calcination process.

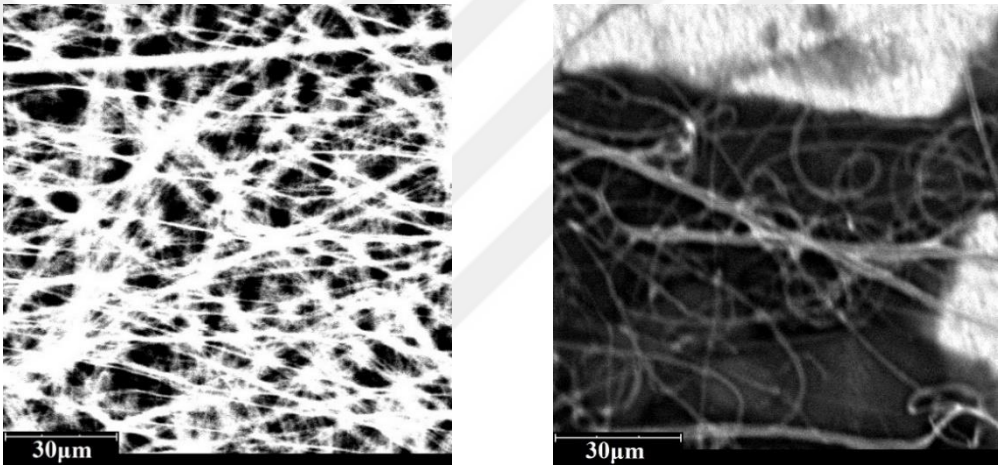

(a) (b)

Figure 3.10 : The SEM images of (a) Sample 2(Eth10) and (b) Sample 2(Eth20) before calcination.

The average diameter of the nanofibers was 1.0813 µm ± 0.2868; which was found coarser than the diameter of regular sample, Sample 2. The reason for obtaining coarser nanofibers was probably the decrease in conductivity due to the addition of ethanol, which was an organic solvent.

3.3.4 The effect of surfactant addition on the structure and electrospinnability

Since no satisfactory results could be obtained in all trials had been made, the effect of surfactant to the solution was also tried. The selection of the surfactant type was very important in terms of the balance between parameters. That is the reason why, a non-ionic type of surfactant “Triton X-100” was chosen (the chemical structure was

shown in Figure 3.11); otherwise, the ionic type of surfactants probably would change the conductivity of the solution and affect the electrospinning performance.

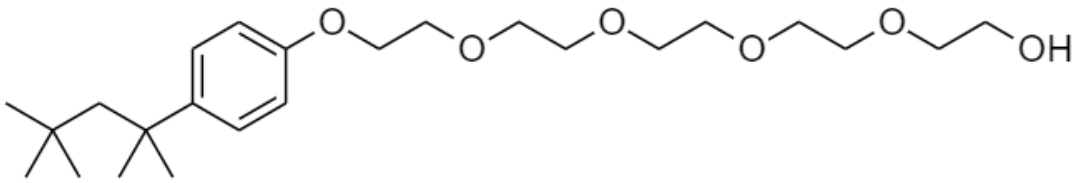

Figure 3.11 : The chemical structure of Triton X-100.

In order to find the ideal surfactant concentration that should be added to a solution, the literature search was done. As a first trial of this work, 10% (w/v) Triton X-100 was added to the solution. The images of the solutions were stated in Figure 3.12 to compare the regular sample and the sample containing surfactant visually.

Figure 3.12 : The result of the visual assessment: A homogeneous zinc acetate dihydrate containing PVA solution with perfectly dissolved surfactant "Triton X-100" (left) and regular sample, Sample 2, (right).

The visual assessment after the preparation of the solution indicated that solution was not transparent, it was blurry. Moreover, it was observed that there were undissolved parts in the solution when it was carefully examined. This was probably due to the change in the solubility behavior of the solvent system, which was presumably caused by the hydrophobic portion of the surfactant. By the addition of the surfactant, a homogeneously dispersed hydrophobicity was introduced to the solvent system. It was concluded that the 10 % (w/v) was not proper concentration, and then solutions were

prepared at various concentrations between 1 % and 10 % (w/v) in order to find the ideal surfactant concentration that offers homogenous solubility. It was found that adding surfactant make the solution blurry regardless of varying concentration. However, the fact that the solution was not transparent did not affect the homogeneity of the solution. Although some undissolved fractions were observed in solutions with higher surfactant concentrations, above 4 % (w/v), it was seen that this was not valid for all concentrations. The solubility of each substance in the solution was great for those samples that had concentration values below 4% (w/v); no undissolved fractions were observed in the solutions.

The electrospinning performances of solutions having surfactant concentration below 4 % (w/v) were also investigated, and it was seen that all solutions performed more or less similar to each other. In this case, the minimum concentration value of 1% was preferred in order to keep minimum the newly formed hydrophobic character of the solution.

The physicochemical studies also confirmed the selection of 1% surfactant concentration was good choice. It was observed that the pH change after the addition of zinc acetate dihydrate for Sample 2(TrX1) was highly identical to the changes seen in regular solution, Sample 2. As stated in previous studies, the measured pH values of the Sample 2 were 5.93 ± 0.009 and 5.92 ± 0.009 after zinc addition and in the final solution, respectively. Table 3.14 indicated that 5.97 ± 0.011 and 5.90 ±0.005 were the pH values of the solution for same stages. The conservation of the pH change could indicate that the formation of $Zn(OH)_2$ through reaction (6) probably occurred with the same efficiency in the surfactant solution.

Table 3.14 : The pH and conductivity results of Sample 2(TrX1) for each preparation step.

Stages	pH	Conductivity (µS/cm)
1- Before $Zn(OAc)_2 \cdot H_2O$ addition	6.47 ± 0.005	8.48 ± 0.045
2- After $Zn(OAc)_2 \cdot H_2O$ addition	5.97 ± 0.011	18235.52 ± 319.95
3- Electrospinning solution	5.90 ±0.005	9460.08 ± 30.36

The conductivity measurements of the Sample 2(TrX1) gave similar results with the regular solutions, except for one point. It was seen that the addition of Triton X-100 reduced the conductivity of distilled water; it was dropped from 28.22 µS/cm ± 0.43

to 8.48 μS/cm ± 0.045. However, conductivity values at the stages of zinc precursor salt addition and electrospinning solution were almost same. Having the zinc acetate dihydrate added; the conductivity value for Sample 2(TrX1) was 18235.52 μS/cm ± 319.95, while it was 18811.02 μS/cm ± 307.89 for regular one. The conductivity value for electrospinning solution of Sample 2(TrX1) was 9460.08 μS/cm ± 30.36; while it was 9788.88 μS/cm ± 47.87 for regular one. These values, which are very close to each other, could even be accepted as coequal to each other. It should be noted that these measurements were not made consecutively on the same day; for this reason, small deviations could be seen. Thus, it can be concluded that 1% surfactant addition had almost no effect on conductivity.

As it is seen in Table 3.15, the viscosity measurement results also indicated that they were highly same as compared to the regular solution results. The corresponding viscosity value for flow rate of 200 uL/min, which is the operational flow rate of Sample 2(TrX1), was 1.786 Pa.s ± 0.039. In the case of Sample 2, the viscosity was 1.71 ± 0.021 for same feed rate; an increase of 4.4% could be considered a negligible difference. Therefore, it can be said that surfactant addition did not considerably affect the viscosity. In fact, this was expected. As it mentioned before; as far as the changes in parameters such as pH were considered, the reaction efficiency of the reaction (6) in the presence of 1% surfactant medium and the reaction efficiency in pure aqueous medium were similar to each other. The remained zinc ions, other products and zinc derivatives that were formed in surfactant solution as a result of reaction (6) were expected to be in almost same quantity as those formed in only distilled water medium. Therefore, the intra- and inter- level interactions between polymer chains that caused by zinc ions and other zinc derivatives were also almost same for both media; which led to get almost similar results for the viscosity.

Table 3.15 : The viscosity chart for Sample 2(TrX1).

	Viscosity Results (Pa.s) for Flow Rate (F.R.)…		
Sample 2(TrX1)	**F.R. 60 uL/min**	**F.R. 100 uL/min**	**F.R. 200 uL/min**
	2.239 ± 0.098	2.077 ± 0.053	1.786 ± 0.039
	F.R. 300 uL/min	**F.R. 400 uL/min**	**F.R. 500 uL/min**
	1.629 ± 0.024	1.604 ± 0.005	1.635 ± 0.015

In these conditions, where the results of all analyzes were more or less the same, it was observed that the factor that made the electrospinning process better was the surface

tension of the solution. While the surface tension measurement result of the Sample 2 was 38.612 mN/m ± 0.881 in Table 3.5; the result of the Sample 2(TrX1), which was the surfactant containing solution, was 31.46 mN/m ± 0.32 in Table 3.16. Probably, approximately 20% decrease in surface tension influenced positively the continuity and stability at the region of taylor cone and jet up to a certain extent; and therefore, better electrospinning performance was observed.

Table 3.16 : The surface tension results of 1% surfactant-containing solutions.

Sample Name	PVA Conc.	$Zn(OAc)_2 \cdot H_2O$ Conc.	Surface Tension (mN/m)
Sample 0(TrX1)	15%	0%	29.22 ± 0.57
Sample 2(TrX1)	15%	15%	31.46 ± 0.32

3.3.4.1 The TGA and SEM analyzes of Sample 2(TrX1)

After the addition of zinc precursor salt to the pure polymer solution sample, some changes were observed in the decomposition performance of Sample 0. After observing this change, the possibility that each new chemical or substance added into the synthesis recipe may cause new changes should be taken into consideration. In the case of investigation made on surfactant solution, the effects of surfactant addition on analyte, Sample 2(TrX1), could obviously be seen in its TGA graph. The effects of the added surfactant in the environment can be understood from the graph at first glance. In the graph that defined in Figure 3.13, four peaks were seen, where the transitions between them were not relatively sharp; they were quite faster. Probably, these new changes were occurred due to the surfactant. As illustrated in Figure 3.11, Triton X-100 has long ethylene oxide units in its hydrophilic side. During the thermal treatment, a smaller fragments of ethylene oxide units could be created, which were supposed to be very reactive [56]. The reactive species formed as the ethylene oxide degraded might trigger each other and be accelerating the degradation of the whole analyte, so that the transitions between peaks were not sharp; proceeded on each other with a relatively less slope difference.

The temperature was around 141.14 °C at the point at which 5 % of the total weight was lost. However, this weight loss was probably referred to water loss; since it was too low compared to the data that was driven from previous findings. If the evaluation of the peaks was carried on, the peak that started at around 215 °C should belonged to

the decomposition of the amorphous regions because that peak was seen sharper than the others. Since the decomposition of amorphous regions were easier, weight loss at that temperature occurred faster. The temperature at the end of this peak was around 275.1 °C and between these temperature points, the weight of the remaining sample decreased from 80.89% to 51.57%. According to the data derived from Figure 3.4, the temperature at which 51.57% of the initial weight of only zinc precursor salt containing sample remained was around 334.76 °C.

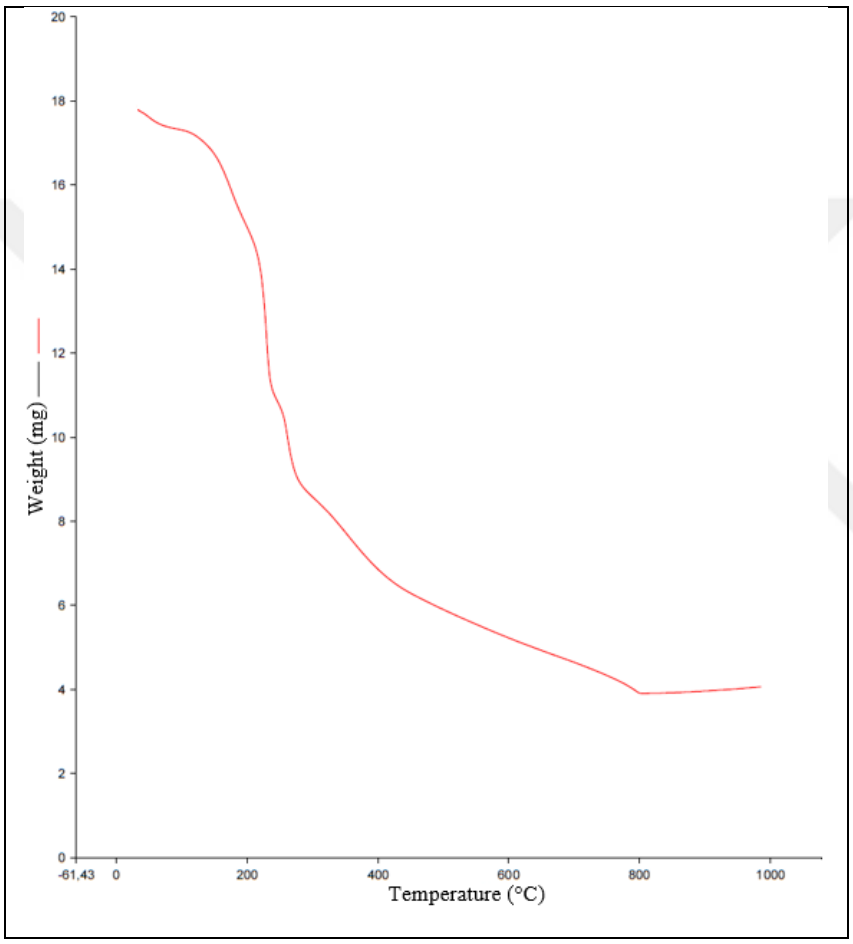

Figure 3.13 : The TGA graph of Sample 2(TrX1).

The further decomposition of PVA and formation of ZnO through reaction (10) occurred simultaneously as seen in previous analysis, and the onset of peak of that was observed at around 418 °C; which continued until 800 °C. Between them, the corresponding temperature for half weight loss, in other words, mid-point of final peak was 594 °C; which was consistent with predetermined temperature point for calcination, 600 °C. At the beginning of the decomposition, 36.9 % of the initial mass

was present in the media, while at the end of the analysis the remaining mass was about 22 %; which belonged to the inorganic residue, ZnO.

The morphological effect of the surfactant addition was also analyzed and SEM images of Sample 2(TrX1) at scale 30 μm and 50 μm could be found in Figure 3.14.

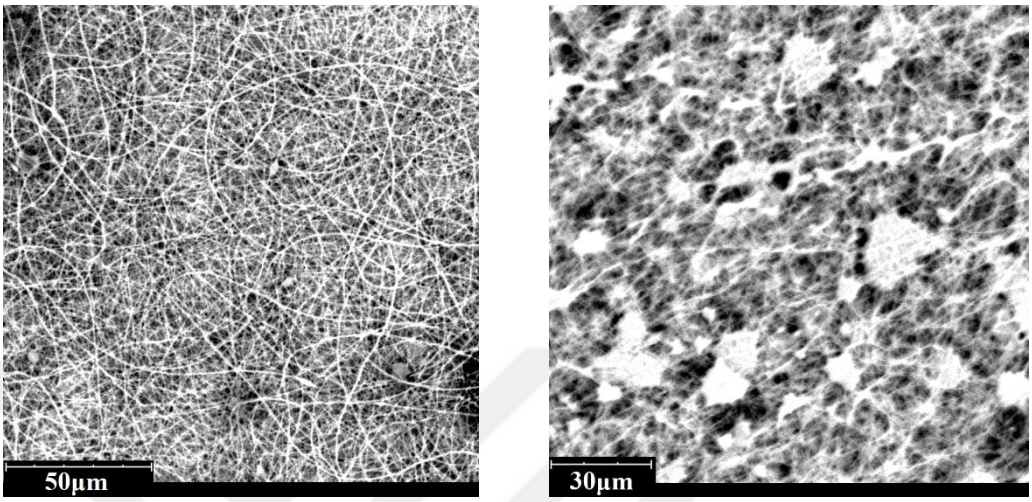

(a) (b)

Figure 3.14 : The SEM images of Sample 2(TrX1); (a) before calcination at scale 50μm and (b) after calcination at scale 30μm.

Based on the data that were derived from the SEM images of Sample 2(TrX1), the average diameter before calcination process was found 0.56 μm ± 0.0802 and the average diameter after calcination process was found 0.31 μm ± 0.08. Both diameter values were found lower than those of Sample 2, 0.870 μm ± 0.173 and 0.632 μm ± 0.09, respectively; so, the addition of 1% surfactant to the Sample 2 led to get finer nanofibers. This is probably due to the decrease in surface tension; since it was less, the requirement for electrostatic forces to overcome the surface tension also decreased. The decrease in surface tension resulted smaller nanofiber diameter, in other words, finer nanofibers.

4. CONCLUSION

In order to achieve the feasible viscosity for electrospinning, the high enough critical concentration value for PVA solution was investigated firstly in this study. Therefore, the PVA solutions in distilled water varying between 7% to 20% (w/v) were prepared and their rheological behavior were investigated through viscosity measurements. Among the prepared samples, the solution having 15% PVA (w/v) concentration was found satisfactory in terms of the polymer chain entanglements.

Then, inorganic precursor zinc acetate dihydrate was added by varying mass ratios 0.5:1, 1:1, 1.5:1 and 2:1 with respect to the 15% PVA solution in order to find the appropriate one. Although viscosity measurements and some physicochemical analyzes such as pH, conductivity and surface tension were performed on all samples, the decision of the proper mass ratio was given by considering the ease of electrospinning operation and the fineness of the fibers since higher surface to volume ratio led to gain higher sensitivity for final product membrane against target NO_x gases. The morphological studies of the nanofibers obtained from each sample were characterized by using SEM, and the corresponding diameter data were measured. The addition of zinc acetate dihydrate led to decrease in pH for all samples, but this decrease was proportional to the amount of the salt added. Probably, the decrease in pH was observed because of the formation of $Zn(OH)_2$ which was thought to be formed by the consumption of hydroxide ions in the environment due to the zinc ions coming from precursor inorganic salt dissolution.

TGA was also performed to determine the calcination temperature of the electrospun sample. Firstly, the only PVA containing sample was calcined in order to define the temperature at which all hydrocarbon content was totally decomposed. It was observed that 95% of the total mass was decomposed at around 600 °C and was completely lost at around 735.3 °C. By considering these data, TGA of the sample containing zinc acetate dihydrate was performed with same annealing conditions in order to examine the effect of precursor zinc salt on decomposition behavior. As a result of the analysis, it was seen that the precursor inorganic salt accelerated the decomposition of the

sample and 16% of the total mass was remained in the environment even at 900 °C. Considering that any hydrocarbon species could not exist at that temperature, it was estimated that the remaining mass belonged to ZnO that was formed by the elimination of water from $Zn(OH)_2$.

Among the electrospun fibers made from solutions with different mass ratios, the results of the solution containing 15% (w/v) PVA and 15% (w/v) zinc acetate dihydrate (labeled as "Sample 2") was chosen for membrane production thanks to its diameter size and electrospinnability. However, Sample 2 needed some improvements on its electrospinnability since the continuity and stability at the region of taylor cone and jet were not found satisfactory enough. That is the reason why, following attempts were applied in order to get a more optimized electrospinning process.

The first attempt was performed in the acidic region. Accordingly, the pH of the electrospinning solution was adjusted to around 3.5 by using acetic acid solution. As a result of visual assessment, the solution prepared in the acidic region, Sample 2(Ac), was as transparent and homogeneous as the regular solution, Sample 2; however, it was observed that the viscosity of the Sample 2(Ac) was 46.87% higher than the viscosity of Sample 2, possibly because of the increased physical interactions.

The studies in basic region was quite difficult because the solubility of $Zn(OH)_2$ was pH and temperature dependent. Since the solubility of $Zn(OH)_2$ was poor around the region where the pH value varies between 8 and 12, it was necessary to work in regions other than this in order to avoid precipitation in solution. In the range where pH was lower than 8, any significant improvements could not be observed. On the other hand, a sharp decrease in viscosity was observed in the region where pH was higher than 12. This decrease was observable with the naked eye because the polymer solution lost its viscosity probably as a result of the repulsion of the deprotonated hydroxyl groups on the PVA chains. Therefore, no results could be obtained from the basic region studies.

The other attempt was performed by using binary solvent system, ethanol and distilled water, since PVA and zinc acetate dihydrate were slightly soluble in pure ethanol. Even some undissolved components were observed in those solutions in which the ethanol concentration in binary solvent system was relatively higher than the water concentration. Thus, only 10% (v/v) and 20% (v/v) ethanol containing solutions were prepared. The visual assessments of the Sample 2(Eth10) and Sample 2(Eth20)

indicated that both solutions were transparent; and therefore, homogeneous. The noticeable change in the physicochemical analyzes performed was the decrease in conductivity depending on the ethanol concentration in the binary solvent system, as organic solvents had lower conductivity than water. As far as the result of Sample 2 compared with the results of Sample 2(Eth10) and Sample 2(Eth20), the conductivity was decreased by approximately 38.84% and 61.95%, respectively. The binary solvent system also affected the viscosity. As the corresponding viscosity results of Sample 2 with respect to the operational flow rate were compared with the results of Sample 2(Eth10) and Sample 2(Eth20); 14.91% increase was observed in former sample and 31.26% increase was observed in latter sample probably due to the increased physical interactions in the medium. Although the electrospinnability of Sample 2(Eth10) was found to be better than the electrospinnability of Sample 2(Eth20), it was not decided to proceed with any samples from the binary solvent system because the average fiber diameter of the fibers obtained from the Sample 2(Eth10) before calcination process was found approximately 24.29% coarser compared to the diameter of Sample 2.

In the last experimental study, a non-ionic surfactant, Triton X-100 was added to the sample in order to investigate the effects on Sample 2. In the experiments carried out to find the ideal surfactant concentration, it was seen that all prepared solutions had become blurry after Triton X-100 addition, regardless of the surfactant concentration. On the other hand, the solubility was adversely affected as the surfactant concentration increased. Among the low concentration group of solutions, it was decided to proceed with 1 % surfactant concentration, taking into account the solution homogeneity and electrospinning performance. The results of all physicochemical analyzes, except surface tension test, and viscosity measurements of Sample 2(TrX1) were notably close to the results of Sample 2. Besides all these results, approximately 20% decrease in surface tension thanks to the surfactant addition was considered the factor affecting the electrospinnability in sufficient manner.

The surfactant addition also affected the decomposition behavior of the sample during the course of thermogravimetric analysis. Probably, the newly formed reactive species through the degradation of the ethylene oxide unit of Triton X-100 enhanced the decomposition of the analyte especially during the degradation of the amorphous regions. The previously determined calcination temperature, 600 °C, was consistent with the calcination performance of the surfactant containing sample, 594 °C. At the

end of the analysis, 22% of the residual mass left and it was not undergone mass loss even after reaching 800 °C. The average fiber diameter of the ZnO fibers obtained from the Sample 2(TrX1) after calcination process was found approximately 50.95% finer compared to the diameter of Sample 2.

The future work of this study will focus to examine the performance of the obtained membrane in gas sensing tests in terms of sensitivity and accuracy. In the case of any unsatisfactory result; it is suggested to add a doping agent to the structure, reduced graphene oxide, in order to increase the sensitivity.

REFERENCES

[1] **Kaloumenou, M. & Skotadis, E. & Lagopati, N. & Efstathopoulos, E. & Tsoukalas, D.** (2022). Breath Analysis: A Promising Tool for Disease Diagnosis—The Role of Sensors. Sensors. 22. 1238. 10.3390/s22031238.

[2] **Mathew, T. & Prabhahari, P. & Nazerin, A. & Pullithadathil, B.** (2015). Technologies for Clinical Diagnosis Using Expired Human Breath Analysis. Diagnostics. 5. 27-60. 10.3390/diagnostics5010027.

[3] **Righettoni, M. & Amann, A. & Pratsinis, S.** (2014). Breath analysis by nanostructured metal oxides as chemo-resistive gas sensors. Materials Today. 18. 10.1016/j.mattod.2014.08.017.

[4] **Mule, N. & Patil, D. & Kaur, M.** (2021). A comprehensive survey on investigation techniques of exhaled breath (EB) for diagnosis of diseases in human body. Informatics in Medicine Unlocked. 26. 100715. 10.1016/j.imu.2021.100715.

[5] **Kharitonov, S. & Barnes, P.** (2001). Exhaled Markers of Pulmonary Disease. American journal of respiratory and critical care medicine. 163. 1693-722. 10.1164/ajrccm.163.7.2009041.

[6] **Miskoff, J. & Dewan, A. & Chaudhri, M.** (2019). Fractional Exhaled Nitric Oxide Testing: Diagnostic Utility in Asthma, Chronic Obstructive Pulmonary Disease, or Asthma-chronic Obstructive Pulmonary Disease Overlap Syndrome. Cureus. 11. 10.7759/cureus.4864.

[7] **Wang, J. & Zhang, W. & Cao, R. & Xiangyu, Y. & Lai, H.** (2016). Analysis of Nitrogen Dioxide in Environment. Advances in Bioscience and Biotechnology. 07. 278-288. 10.4236/abb.2016.76026.

[8] **Minissale, M. & Congiu, E & Baouche, S. & Chaabouni, H. & Moudens, A. & Dulieu, F. & Manicó, G. & Pirronello, A.** (2013). Formation of nitrogen oxides via NO + O2 gas–solid reaction on cold surfaces. Chemical Physics Letters. 565. 52–55. 10.1016/j.cplett.2013.02.028.

[9] **Franke, M. & Koplin, T. & Simon, U.** (2006). Metal and Metal Oxide Nanoparticles in Chemiresistors: Does the Nanoscale Matter?. Small (Weinheim an der Bergstrasse, Germany). 2. 36-50. 10.1002/smll.200500261.

[10] **Sopiha, K. & Malyi, O. & Persson, C. & Wu, P.** (2021). Chemistry of Oxygen Ionosorption on SnO 2 Surfaces. ACS Applied Materials & Interfaces. XXXX. 10.1021/acsami.1c08236.

[11] **Hayyan, M. & Hashim, M. & Alnashef, I.** (2016). Superoxide Ion: Generation and Chemical Implications. Chemical Reviews. 116. 10.1021/acs.chemrev.5b00407.

[12] **Yamazoe, N. & Shimanoe, K.** (2013). Fundamentals of semiconductor gas sensors. Semiconductor gas sensors (1st edition), pp (3-38), Woodhead Publishing.

[13] **Kołodziejczak-Radzimska, A. & Jesionowski, T.** (2014). Zinc Oxide—From Synthesis to Application: A Review. Materials. 7. 10.3390/ma7042833.

[14] **Iwan, S. & Dianisya, D & Isnaeni, I.** (2018). Crystal structure analyses of ZnO nanoparticles growth by simple wet chemical method. IOP Conference Series: Materials Science and Engineering. 434. 012077. 10.1088/1757-899X/434/1/012077.

[15] **Yanda Shaba, E. & Jacob, J. & Tijani, J. & Suleiman, M.** (2021). A critical review of synthesis parameters affecting the properties of zinc oxide nanoparticle and its application in wastewater treatment. Applied Water Science. 11. 48. 10.1007/s13201-021-01370-z.

[16] **Korotcenkov, G.** (2021). Electrospun Metal Oxide Nanofibers and Their Conductometric Gas Sensor Application. Part 1: Nanofibers and Features of Their Forming. Nanomaterials. 11. 1544. 10.3390/nano11061544.

[17] **Wang, M & Zhou, Y. & Zhang, Y. & Hahn, S. & Kim, E.** (2011). From $Zn(OH)_2$ to ZnO: A study on the mechanism of phase transformation. CrystEngComm. 13. 6024-6026. 10.1039/C1CE05502J.

[18] **Kollarigowda, R. & Kizhakke Veettil, S. & Thakur, P.** (2022). Approaches to Preceramic Polymer Fiber Fabrication and On-Demand Applications. Materials. 15. 4546. 10.3390/ma15134546.

[19] **Qu, G. & Fan, G. & Zhou, M. & Rong, X. & Li, T. & Zhang, R. & Sun, J. & Chen, D.** (2019). Graphene-Modified ZnO Nanostructures for Low-Temperature NO_2 Sensing. ACS Omega. 4. 4221-4232. 10.1021/ acsomega.8b03624.

[20] **Silva, E. & Oliveira, V. & Marques, V. & Rubira, A. & Silva, R. & Cava, C. & Lourenço, S. & Muniz, E.** (2020). Electrospun fibers of poly (vinyl alcohol): zinc acetate (PVA:AcZn) and further ZnO production: evaluation of PVA:AcZn ratio and annealing temperature effects on ZnO structure. Journal of Nanoparticle Research. 10.1007/s11051-020-05048-6

[21] **Guisbiers, G. & Mejía-Rosales, S. & Francis, L.** (2012). Nanomaterial Properties: Size and Shape Dependencies. Journal of Nanomaterials. 2012. 10.1155/2012/180976.

[22] **Ganesan, A. & Rengarajan, J.** (2022). A review on fabrication methods of nanofibers and a special focus on application of cellulose nanofibers. Carbohydrate Polymer Technologies and Applications. 4. 100262. 10.1016/j.carpta.2022.100262.

[23] **Muthukrishnan, L.** (2022). An overview on electrospinning and its advancement toward hard and soft tissue engineering applications. Colloid and Polymer Science. 300. 1-27. 10.1007/s00396-022-04997-9.

[24] **Fang, Q. & Zhu, M. & Yu, S. & Sui, G. & Yang, X.** (2016). Studies on soy protein isolate/polyvinyl alcohol hybrid nanofiber membranes as multi-

functional eco-friendly filtration materials. Materials Science and Engineering: B. 214. 10.1016/j.mseb.2016.08.004.

[25] **Hong, J. & Yeo, M. & Yang, G. H. & Kim, G.** (2019). Cell-Electrospinning and Its Application for Tissue Engineering. International Journal of Molecular Sciences. 20. 6208. 10.3390/ijms20246208.

[26] **Keirouz, A. & Wang, Z. & Reddy, V. & Nagy, Z. & Vass, P. & Buzgo, M. & Ramakrishna, S. & Radacsi, N.** (2023). The History of Electrospinning: Past, Present, and Future Developments. 8. 10.1002/admt.202201723.

[27] **Long Y.Z., Yan X., Wang X.X., Zhang J., Yu M.** Chapter 2 - Electrospinning: The Setup and Procedure. Editor(s): Ding B., Wang X. and Yu J. In Micro and Nano Technologies, "Electrospinning: Nanofabrication and Applications", William Andrew Publishing, 2019, Pages 21-52, ISBN 9780323512701.

[28] **Garg, K. & Bowlin, G.** (2011). Electrospinning Jets and Nanofibrous Structures. Biomicrofluidics. 5. 13403. 10.1063/1.3567097.

[29] **Robb B., Lennox B.** Chapter 3 - The electrospinning process, conditions and control, Editor(s): Bosworth L.A., Downes S., In Woodhead Publishing Series in Biomaterials, "Electrospinning for Tissue Regeneration", Woodhead Publishing, 2011, Pages 51-66, ISBN 9781845697419.

[30] **Haider, A. & Haider, S. & Kang, I.K.** (2015). A comprehensive review summarizing the effect of electrospinning parameters and potential applications of nanofibers in biomedical and biotechnology. Arabian Journal of Chemistry. 11. 10.1016/j.arabjc.2015.11.015.

[31] **Amariei, N. & Manea, L. & Bertea, A. & Bertea, A. P. & Popa, A.** (2017). The Influence of Polymer Solution on the Properties of Electrospun 3D Nanostructures. IOP Conference Series: Materials Science and Engineering. 209. 012092. 10.1088/1757-899X/209/1/012092.

[32] **Ewaldz, E. & Randrup, J. & Brettmann, B.** (2021). Solvent Effects on the Elasticity of Electrospinnable Polymer Solutions. ACS Polymers Au. XXXX. 10.1021/acspolymersau.1c00041.

[33] **Al-Abduljabbar, A. & Farooq, I.** (2022). Electrospun Polymer Nanofibers: Processing, Properties, and Applications. Polymers. 15. 65. 10.3390/polym15010065.

[34] **He, H. & Kara, Y. & Molnar, K.** (2018). Effect of needle characteristic on fibrous PEO produced by electrospinning. Resolution and Discovery. 4. 1-5. 10.1556/2051.2018.00063.

[35] **Gao, H.W. & Yang, R.J. & He, J.Y. & Yang, L.** (2009). Rheological Behaviors of PVA/H2O Solutions of High-Polymer Concentration. Journal of Applied Polymer Science. 116. 1459 - 1466. 10.1002/app.31677.

[36] **Jamnongkan, T. & Shirota, R. & Sukumaran, S. & Sugimoto, M. & Koyama, K.** (2013). Effect of ZnO Nanoparticles on the Electrospinning of Poly(vinyl alcohol) From Aqueous Solution: Influence of Particle Size. Polymer Engineering & Science. 54. 10.1002/pen.23730.

[37] **Leach, M. & Feng, Z.-Q. & Tuck, S. & Corey, J.** (2011). Electrospinning Fundamentals: Optimizing Solution and Apparatus Parameters. Journal of visualized experiments: JoVE. 47. 10.3791/2494.

[38] **Abbasipour, M. & Khajavi, R.** (2017). Controlling nanofiber morphology by the electrospinning process. 10.1016/B978-0-08-100907-9.00005-2.

[39] **Reichle, R. & McCurdy, K. & Hepler, L.** (1975). Zinc Hydroxide: Solubility Product and Hydroxy-Complex Stability Constants from 12.5-75°C. Canadian Journal of Chemistry. 53. 3841-3845. 10.1139/v75-556.

[40] **Angammana, C. & Jayaram, S.** (2011). Analysis of the Effects of Solution Conductivity on Electrospinning Process and Fiber Morphology. Industry Applications, IEEE Transactions on. 47. 1109 - 1117. 10.1109/TIA.2011.2127431.

[41] **Islam, M. S.l & Ang, B. & Andriyana, A. & Ma, A.** (2019). A review on fabrication of nanofibers via electrospinning and their applications. SN Applied Sciences. 1. 10.1007s42452-019-1288-4.

[42] **Bhattacharya, A. & Ray, P.** (2004). Studies on surface tension of poly(vinyl alcohol): Effect of concentration, temperature, and addition of chaotropic agents. Journal of Applied Polymer Science. 93. 122 - 130. 10.1002/app.20436.

[43] **Park, J.C. & Ito, T. & Kim, K.O. & Kim, K. & Kim, B.S. & Khil, M. & Kim, H. & Kim, I.S.** (2010). Electrospun poly(vinyl alcohol) nanofibers: Effects of degree of hydrolysis and enhanced water stability. Polymer Journal. 42. 10.1038/pj.2009.340.

[44] **Natale, D. & Mareque-Rivas, J.** (2008). ChemInform Abstract: The Combination of Transition Metal Ions and Hydrogen-Bonding Interactions. Chemical communications (Cambridge, England). 39. 425-37. 10.1039/b709650j.

[45] **Zhang, Y. & Li, H. & Li, C. & Chen, X. & Lesser, A.** (2018). Investigation of "Zn^{2+} salt-bondings" cross linked ENR with shape memory effect via ionic interactions: Zn2+ Salt-Bondings Cross Linked ENR. Polymer Engineering & Science. 59. 10.1002/pen.24989.

[46] **Naseem, B., Arif, I., & Jamal, M. A.** (2021). Kosmotropic and chaotropic behavior of hydrated ions in aqueous solutions in terms of expansibility and compressibility parameters. Arabian Journal of Chemistry, 14(11), 103405. doi:10.1016/j.arabjc.2021.103405

[47] **Fedotova, M. V., & Kruchinin, S. E.** (2011). Hydration of acetic acid and acetate ion in water studied by 1D-RISM theory. Journal of Molecular Liquids, 164(3), 201–206. doi:10.1016/j.molliq.2011.09.015

[48] **Petit, T. & Aziz-Lange, K. & Conrad, G. & Yamamoto, K. & Schwanke, C. & Hodeck, K. & Dantz, M. & Brandenburg, T. & Suljoti, E. & Aziz, E.** (2014). Probing ion-specific effects on aqueous acetate solutions: Ion pairing versus water structure modifications. Structural Dynamics. 10.1063/1.4884600.

[49] **Sanchez Y. (2020).** TA Instruments Applications Organization. “Estimation of Polymer Lifetime by TGA Decomposition Kinetics”. Retrieved (Aug 2023) from https://www.tainstruments.com/pdf/literature/ta125.pdf

[50] **Kayani, Z. & Saleemi, F. & Batool, I.** (2015). Effect of calcination temperature on the properties of ZnO nanoparticles. Applied Physics A. 119. 10.1007/s00339-015-9019-1.

[51] **Espitia, P. & Soares, N. & Coimbra, J. & Andrade, N. & Cruz, R. & Medeiros, E.** (2012). Zinc Oxide Nanoparticles: Synthesis, Antimicrobial Activity and Food Packaging Applications. Food and Bioprocess Technology. 5. 10.1007/s11947-012-0797-6.

[52] **Briscoe, B. & Luckham, P. & Zhu, S.** (2000). The effects of hydrogen bonding upon the viscosity of aqueous poly(vinyl alcohol) solutions. Polymer. 41. 3851-3860. 10.1016/S0032-3861(99)00550-9.

[53] **Darabi, M.A. & Khosrozadeh, A. & Wang, Y. & Ashammakhi, N. & Alem, H. & Erdem, A. & Chang, Q. & Xu, K. & Liu, Y. & Luo, G. & Khademhosseini, A. & Xing, M.** (2020). An Alkaline Based Method for Generating Crystalline, Strong, and Shape Memory Polyvinyl Alcohol Biomaterials. Advanced Science. 10.1002/advs.201902740.

[54] **Marín, E. & Rojas, J. & Ciro, Y.** (2014). Polyvinyl alcohol derivatives: Promising materials for pharmaceutical and biomedical applications. Afr J Pharm Pharmacol. 8. 674-684.

[55] **Zaitoon, A. & Lim, L.T.** (2020). Effect of Poly(ethylene oxide) on the Electrospinning Behavior and Characteristics of Ethyl Cellulose Composite Fibers. Materialia. 10.100649.10.1016/j.mtla.2020.100649.

[56] **Čović, A. & Vrandečić, N.** (2021). Influence of poly(ethylene oxide) sample preparation on the results of thermogravimetric analysis. St open. 2. 1-13. 10.48188/so.2.5.

APPENDICES

APPENDIX A: Fiber Diameter Analysis Results

APPENDIX A

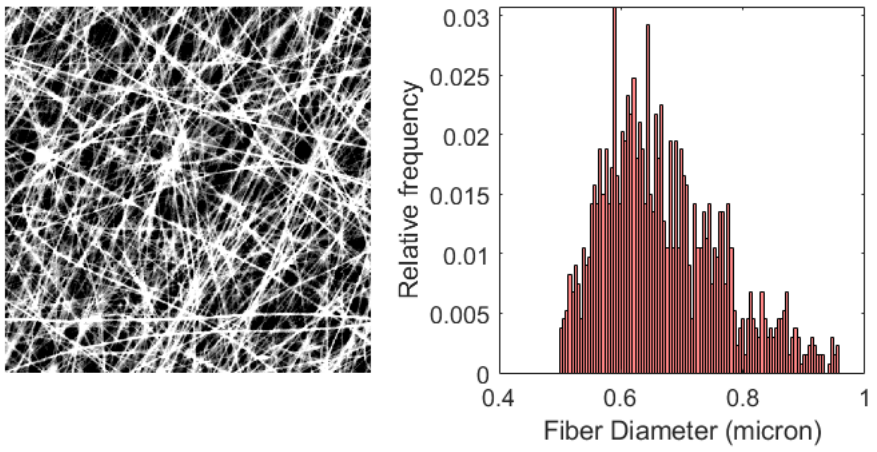

(a)

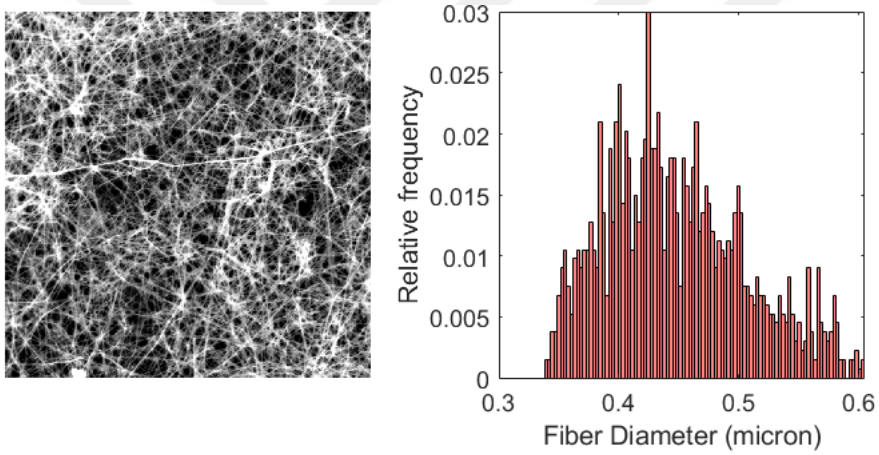

(b)

Figure A.1 : The fiber diameter analysis of Sample 1; before (a) and after (b) calcination at scale 30μm.

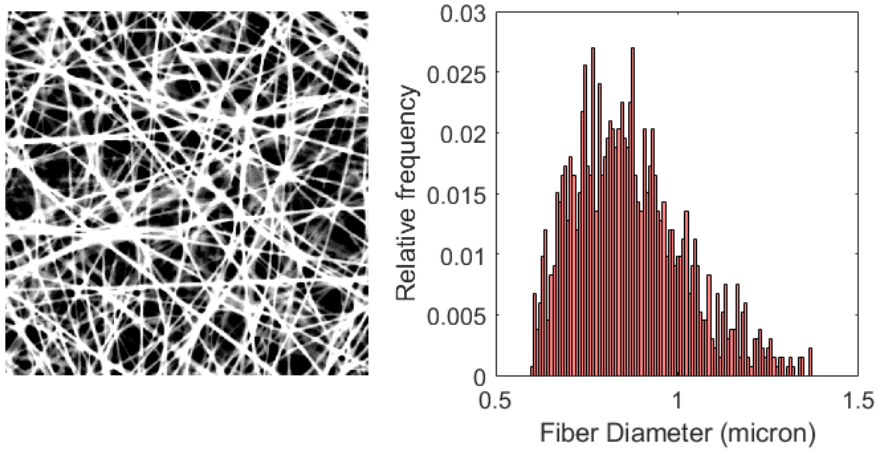

(a)

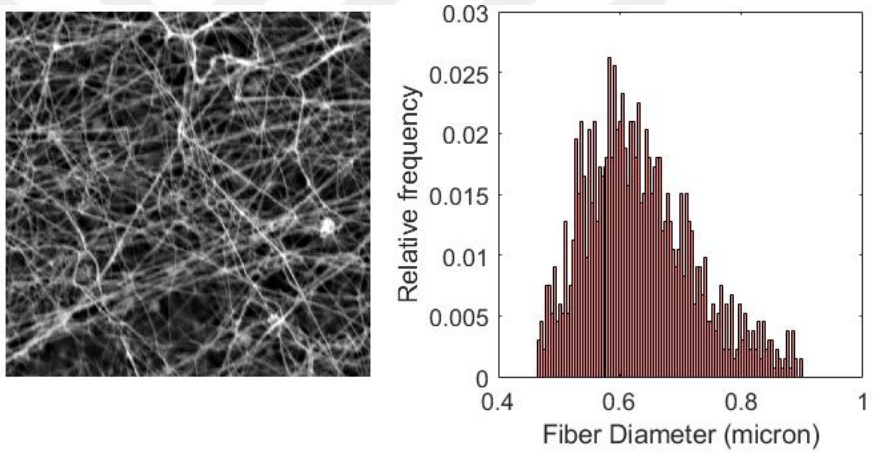

(b)

Figure A.2 : The fiber diameter analyzed of Sample 2; before (a) and after (b) calcination at scale 30μm.

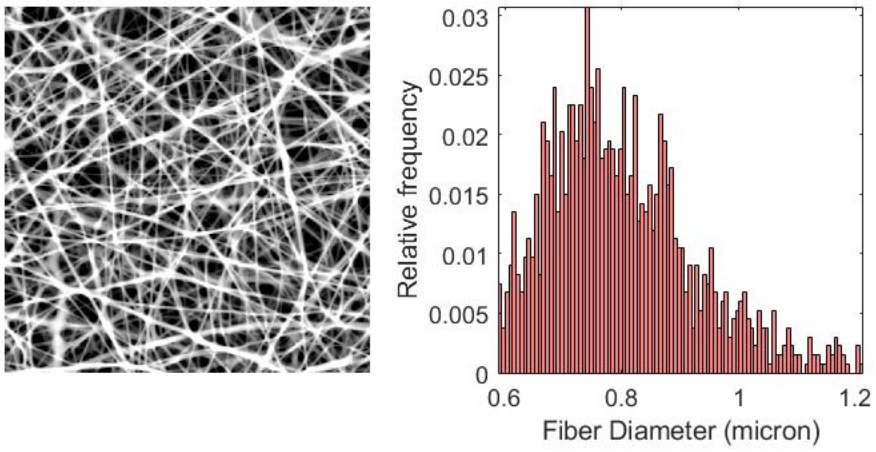

(a)

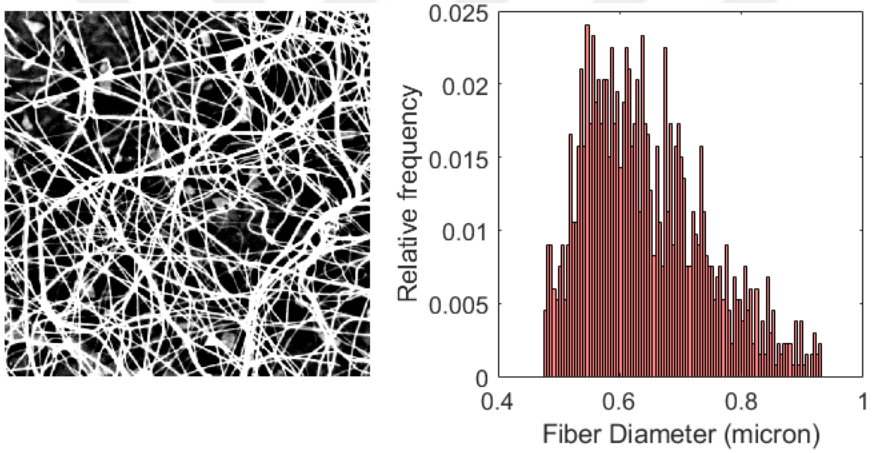

(b)

Figure A.3 : The fiber diameter analyzes of Sample 3; before (a) and after (b) calcination at scale 30μm.

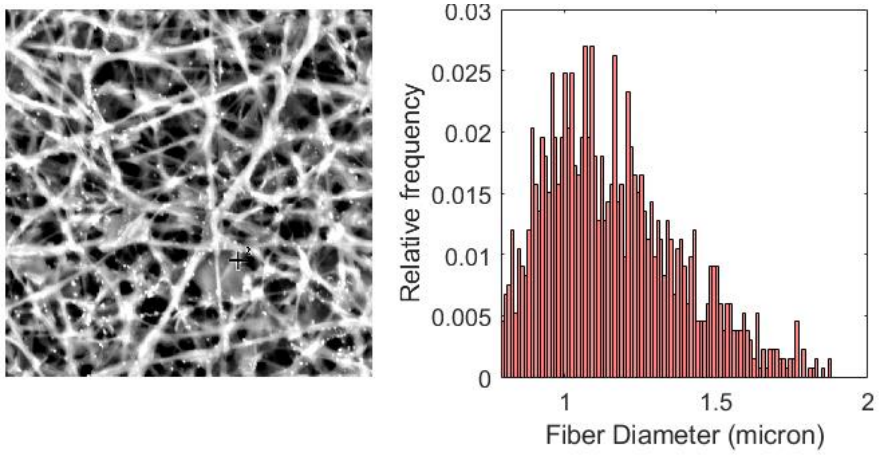

(a)

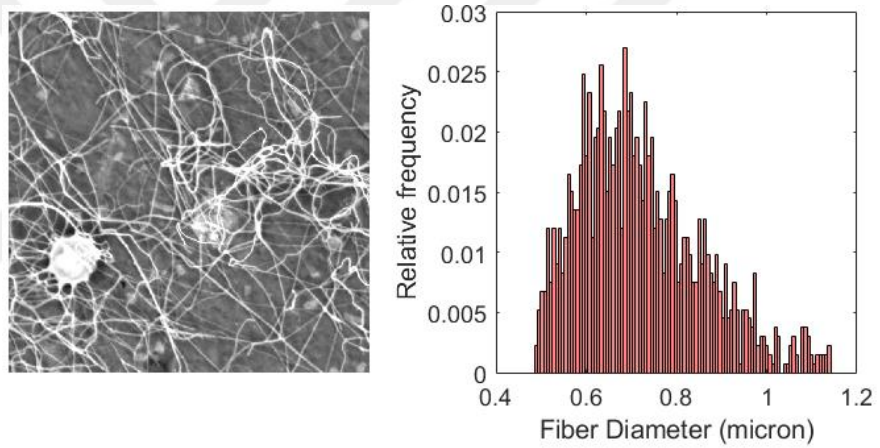

(b)

Figure A.4 : The fiber diameter analyzes of Sample 4; before (a) and after (b) calcination at scale 30μm.

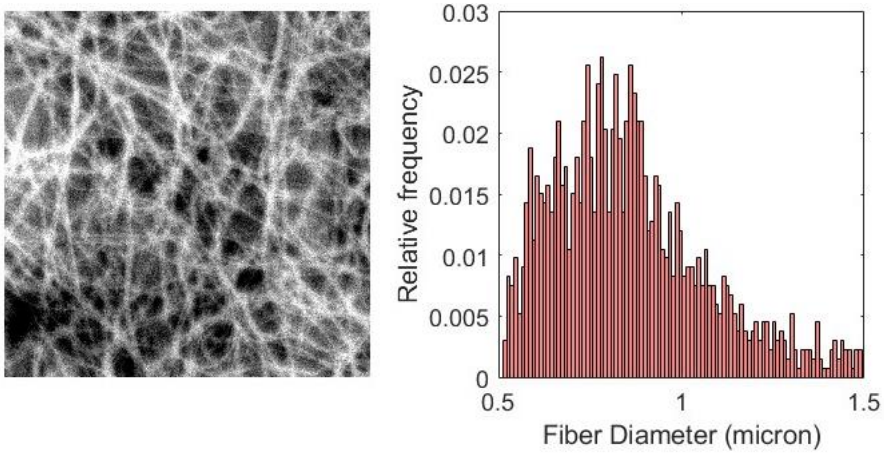

Figure A.5 : The fiber diameter analysis of Sample 2(Ac) before calcination at scale 50μm.

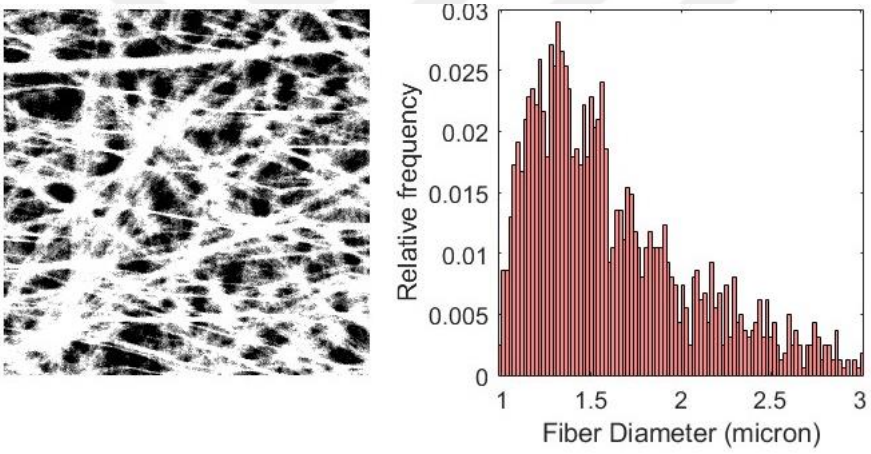

Figure A.6 : The fiber diameter analysis of Sample 2(Eth10) before calcination at scale 30μm.

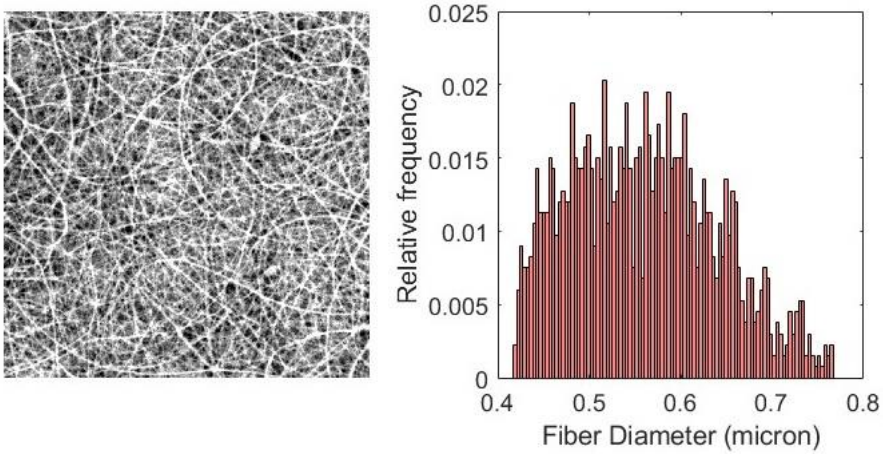

Figure A.7 : The fiber diameter analysis of Sample 2(TrX1) before calcination at scale 50μm.

CURRICULUM VITAE

Name Surname **:** Ari HAKGÖR

EDUCATION **:**

- **B.Sc.** **:** 2008, Kocaeli University, Faculty of Arts and Sciences, Department of Chemistry
- **M.Sc.** **:** 2018, Boğaziçi University, Institute of Graduate Studies in Science & Engineering, Department of Chemistry

PUBLICATIONS, PRESENTATIONS AND PATENTS ON THE THESIS:

- **Hakgor, A.**, Eryuruk, S. H., (2023). Development of a Gas Sensing Membrane for Asthma Detection. 2nd International Graduate Research Symposium - IGRS'23, 16-18 May 2023 Istanbul – Türkiye.

OTHER PUBLICATIONS, PRESENTATIONS AND PATENTS:

- **Hakgor, A.**, Erol Gunal, S., (2021). Energy barriers to rotation in axially chiral quinazoline-4-ones. Tetrahedron. 100.132506.10.1016/j.tet.2021.132506.